GEOLOGY

Orographic evolution of northern Tibet shaped vegetation and plant diversity in eastern Asia

Shu-Feng Li[1,2,3]*, Paul J. Valdes[3], Alex Farnsworth[3], T. Davies-Barnard[3,4,5], Tao Su[1,2], Daniel J. Lunt[3], Robert A. Spicer[1,6], Jia Liu[1], Wei-Yu-Dong Deng[1,7], Jian Huang[1], He Tang[1,7], Andy Ridgwell[3,8], Lin-Lin Chen[1,7], Zhe-Kun Zhou[1,9]*

The growth of the Tibetan Plateau throughout the past 66 million years has profoundly affected the Asian climate, but how this unparalleled orogenesis might have driven vegetation and plant diversity changes in eastern Asia is poorly understood. We approach this question by integrating modeling results and fossil data. We show that growth of north and northeastern Tibet affects vegetation and, crucially, plant diversity in eastern Asia by altering the monsoon system. This northern Tibetan orographic change induces a precipitation increase, especially in the dry (winter) season, resulting in a transition from deciduous broadleaf vegetation to evergreen broadleaf vegetation and plant diversity increases across southeastern Asia. Further quantifying the complexity of Tibetan orographic change is critical for understanding the finer details of Asian vegetation and plant diversity evolution.

INTRODUCTION

Mountain uplift can markedly alter climate systems, potentially driving vegetation dynamics and species diversification, and may be fundamental for creating exceptional biodiversity (*1*). During the Cenozoic (the past 66 Ma), Tibetan orographic changes profoundly modified regional and global climate (*2*), potentially altering large-scale vegetation and biodiversity over Asia (*3*). This region of unparalleled Cenozoic orogenesis today hosts globally extraordinary biodiversity (*4*), making it ideal for exploring in more detail the links between orographic evolution, climate, vegetation, and biodiversity.

Rich sedimentary and fossil records indicate a broad arid climate zone extended east-west across China throughout the Paleogene (*5*, *6*). This arid belt was superseded by a more humid zone during the Neogene, with some gradual drying toward the present (*5*, *6*). Consequently, vegetation changed from deciduous broadleaf forest to evergreen broadleaf forest in southeastern Asia (fig. S1 and data S1), and the arid/semiarid vegetation belt retreated to the northwest of eastern Asia (fig. S2 and data S1) (*5*, *6*). Recent phylogenetic advances also indicate that many plant lineages in eastern China only diversified after the start of the Miocene (~23 Ma), and modern plant diversity only became established there in the late Cenozoic (*7*, *8*). Previous studies argue that the rise of the Tibetan Plateau intensified the Asia monsoon system (*9*–*11*) and potentially drove species diversification and vegetation change (*3*, *7*, *8*). However, because the history of Tibetan orogenic growth and by extension the Asian climate system is now known to be more complex than simple monolithic plateau uplift [Fig. 1; (*11*–*13*)], the underlying mechanisms of how Tibetan orogeny affected climate and associated vegetation/biodiversity changes in eastern Asia remain unresolved.

Numerical modeling is a powerful tool for exploring links between long-term orogenesis, climate change, and associated vegetation dynamics. However, classic climate sensitivity simulations treat Tibet as a single geological unit with no spatial complexity changing its height against a background of present- or paleogeography (*14*–*17*). Some studies have simulated complex regional uplift histories (*10*, *18*), but very few modeling studies have directly examined the impact of Tibetan development on vegetation (*19*, *20*) and none on biodiversity. Therefore, the links between the evolution of Tibetan topography and vegetation/biodiversity changes across eastern Asia are still poorly understood.

Three key issues are unsolved in this context: (i) In what ways did successive Tibetan orogenic events affect climate? (ii) Why did vegetation and biodiversity change in eastern Asia so markedly from the late Paleogene to early Neogene? (iii) How were these changes coupled to Tibetan orogeny?

We conduct 18 sensitivity experiments (fig. S3 and data S2) using different Tibetan topographies representing various late Paleogene to early Neogene conditions, which test almost all possible Tibetan orographic evolution scenarios (*3*, *12*, *13*, *21*–*23*). We use the atmosphere model, HadAM3 [specifically HadAM3B-M2.1aD as described by Valdes *et al.* (*24*), with a resolution of 3.75° × 2.5° longitude and latitude], and use the Chattian baseline paleogeography [the Late Oligocene, 27.8 to 23.0 Ma, described by Lunt *et al.* (*25*)]. Using a fully coupled atmosphere-ocean general circulation model (GCM), Lunt *et al.* (*19*) have shown that the sea surface temperatures (SSTs) to the east and south of Asia are essentially insensitive to Tibetan orogeny, so ocean circulation variations caused by topographic changes can be excluded. Therefore, to focus on differentiating topography-induced climatic changes, we use the atmospheric HadAM3 model with prescribed SSTs from previous fully coupled atmosphere GCM simulations (*11*). We use the GCM to drive the Sheffield dynamic global vegetation model (SDGVM) (*26*) for vegetation simulations and the Jena Diversity-Dynamic Global Vegetation Model (JeDi-DGVM) (*27*) to explore plant diversity (represented by functional richness; see Materials and Methods). We select four simulations (see Supplementary Text for details)

[1]CAS Key Laboratory of Tropical Forest Ecology, Xishuangbanna Tropical Botanical Garden, Chinese Academy of Sciences, Mengla 666303, China. [2]Center of Plant Ecology, Core Botanical Gardens, Chinese Academy of Sciences, Mengla 666303, China. [3]School of Geographical Sciences, University of Bristol, Bristol, UK. [4] College of Engineering, Maths, and Physical Sciences, University of Exeter, Exeter, UK. [5]Max Planck Institute for Biogeochemistry, Jena, Germany. [6]School of Environment, Earth and Ecosystem Sciences, The Open University, Milton Keynes, MK7 6AA, UK. [7]University of Chinese Academy of Sciences, Beijing 100049, China. [8]Earth and Planetary Sciences, University of California, Riverside, CA 92521, USA. [9]Key Laboratory of Biogeography and Biodiversity, Kunming Institute of Botany, Chinese Academy of Sciences, Kunming 650204, China.
*Corresponding author. Email: lisf@xtbg.org.cn (S.-F.L.); zhouzk@xtbg.ac.cn (Z.-K.Z.)

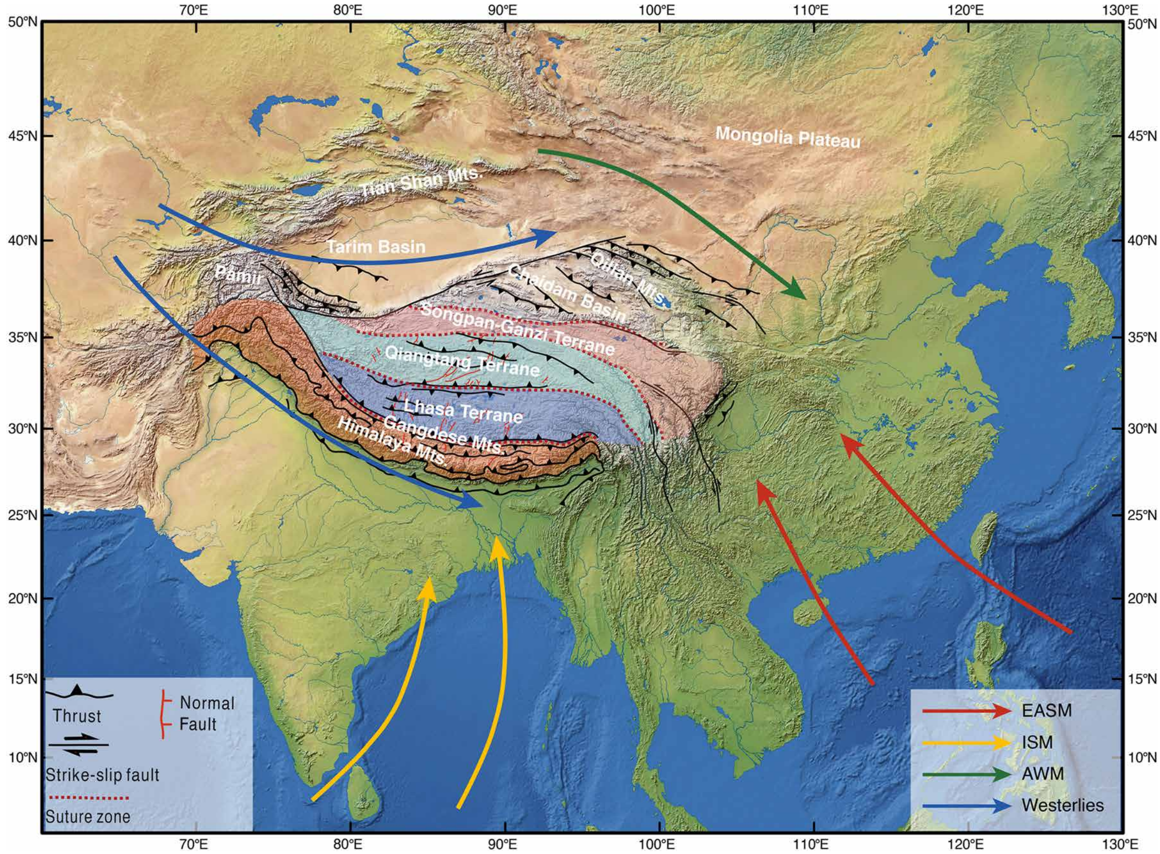

Fig. 1. Modern major tectonic terranes and features of the Himalaya-Tibetan Plateau regions and Asian climate system. From north to south Tibet comprises the Qilian, Kunlun-Qaidam, Songpan-Ganzi, Qiangtang, and Lhasa terranes (including the Gangdese Mountains) separated by suture zones, with the Himalaya to the south. The Asian climate system encompasses the East Asian summer monsoon (EASM), Indian summer monsoon (ISM), Asian winter monsoon (AWM), and westerlies.

for the purpose of comparing the simulated SDGVM results (fig. S4) with paleobotanical data (fig. S1 and data S1) (*5*, *6*) to examine the consequences of orographic development in key parts of Tibet (Fig. 1).

RESULTS AND DISCUSSION

Our results reveal a fundamental linkage between Tibetan orographic evolution, climate, and the development of vegetation/plant diversity in eastern Asia (here, we mainly focus on China because of its rich Cenozoic fossil record). The simulated SDGVM results show when the Gangdese Mountains and Lhasa Terrane were high (Fig. 2, A1 and A2, and fig. S3, J and K), deciduous broadleaf forests covered large areas of eastern Asia, and evergreen broadleaf taxa occurred only sparsely (Fig. 2, B1 and B2, and fig. S4, J and K). This outcome is similar to the simulated SDGVM results for low Tibet scenarios (fig. S4, B to D and G). Under these conditions, plant diversity remained quite low in eastern Asia (Fig. 2, C1 and C2). By contrast, when northern (Qiangtang) and northeastern (Songpan-Ganzi) terranes (Fig. 2, A3 and A4, and fig. S3, L to O) were elevated, vegetation changed markedly from deciduous broadleaf to evergreen broadleaf across a large region of eastern Asia (around 20°N to 35°N; Fig. 2, B3 and B4, and fig. S4, L to O). Functional richness increased correspondingly in southeastern Tibet and southeastern Asia when Tibet grew northeastward (Fig. 2, C1 to C4). Specifically, the rise of the Songpan-Ganzi Terrane produced the greatest plant diversity increase in east China (Fig. 2, C4) and an eastern Asia plant diversity pattern resembling that of today (*4*). Note that when the central part of Tibet is elevated above 3000 m (fig. S3, E, F, H, and I), a threshold-like transition from deciduous broadleaf to evergreen broadleaf vegetation presented in southeastern Asia (fig. S4, E, F, H, and I).

The simulated vegetation and plant diversity change patterns resemble closely fossil, geologic, and phylogenetic data (figs. S1 and S2, and data S1). The reconstructed vegetation types as defined in the SDGVM derived from pollen and megafossil records indicate deciduous broadleaf vegetation types covered large areas of southeastern Asia during the Paleogene, while the evergreen broadleaf vegetation dominated across southeastern Asia in the Neogene (fig. S1). In the northeast China, the reconstructed vegetation maps show the dominant vegetation was deciduous broadleaf type so broadly consistent with the simulated results. Although large areas of evergreen broadleaf vegetation appeared in the Paleocene in northeast China (fig. S1A), this is not present in the low Tibet simulations (fig. S4, B to D and G). In the northwest part of eastern Asia, paleobotanical records show that vegetation was mainly composed with a mixed grassland and deciduous broadleaf types (fig. S1), generally matching the simulations (fig. S4).

Figure S2 indicates a latitude-parallel broad expanse of arid or semiarid vegetation extending across China during the Paleogene, while in the Neogene eastern China hosted humid forests (*5*, *6*). Because precipitation is a key factor determining the growth and, particularly, the phenology of plants and the distribution of vegetation in middle and low latitudes of east Asia (~20°N to 35°N) (*28*), deciduous

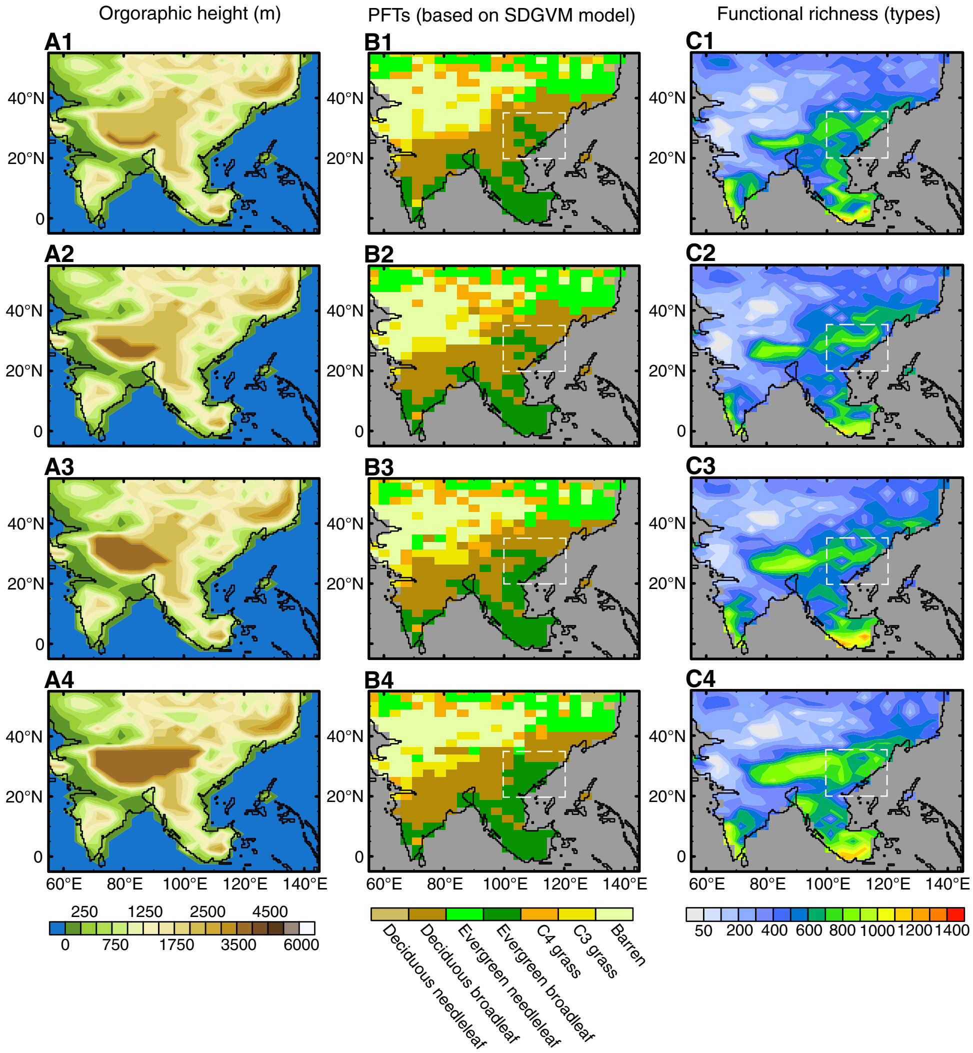

Fig. 2. Four different Tibetan topographic conditions, simulated vegetation and plant diversity. Paleotopographies (data S2) are shown in (**A1**) to (**A4**). (**B1**) to (**B4**) show simulated vegetation results from the SDGVM. (**C1**) to (**C4**) show simulated plant diversity results from the JeDi-DGVM. The white dashed boxes indicate the East Asia region (100°E to 120°E, 20°N to 35°N) discussed in the main text. The brown arc in A1 represents the Gangdese Mountains, which existed before the rise of the Himalaya (*21*). See Supplementary Text for more details for the selection of four simulations.

broadleaf forest can be reasonably treated as arid/semiarid vegetation type and the predominance of evergreen broadleaf plants as reflecting humid/semi-humid conditions in southeastern Asia. However, in northeast China, the winter temperature is more important than precipitation for plants, and cold plays an important role in determining whether leaves are retained year-round or not (*28*). In that region, deciduous broadleaf forests normally represent humid/semihumid vegetation types, but where frozen soils limit plant access to water in winter and as indicated by fossil records (*5*, *6*) and present climate conditions. On the basis of the above discussion, the present results reveal that the two different reconstructed vegetation results (figs. S1 and S2) are generally consistent. Sedimentary records similarly show the environment of eastern China changed across the Paleogene to Neogene transition from arid as indicated by red beds and evaporites, including gypsum, halite, and glauberite to humid as represented by oil shales and coals (*5*, *6*). Recent advances in phylogenetic reconstructions have indicated that many plant taxa (including numerous essential elements in subtropical evergreen broadleaf forests such as Fagaceae, Theaceae, Magnoliaceae, and Lauraceae) in eastern China diversified after the Oligocene/Miocene boundary, and modern plant diversity arose in the late Cenozoic (*7*, *8*, *29*). This phylogenetic pattern generally agrees with the simulated plant diversity changes showing that the plant functional types increased progressively as the Tibet developed northeastward (Fig. 2, C1 to C4).

These Neogene changes in diversification and vegetation modernization in eastern Asia contrast with a growing body of evidence that shows earlier changes in southwestern China. Previous studies (*5*–*8*) have argued that vegetation and biodiversity changes were simply driven by changes in the summer monsoon caused by the unified rise of Tibet at the Oligocene/Miocene boundary. However, some parts of the Tibetan region were already high before the Oligocene (*12*, *13*, *21*, *23*, *30*, *31*), and it is in some parts of southwestern China that we see vegetation and biodiversity patterns

(Fig. 2, B1, B2, C1, and C2) modernizing before the end of the Paleogene (*32*).

The key driver of the transition from deciduous broadleaf to evergreen broadleaf vegetation in eastern Asia is the dry season precipitation. The driest season [December, January, and February (DJF), winter] and wettest season [June, July, and August (JJA), summer] precipitation increased as northern Tibet rose (Fig. 3). The largest percentage increase is in the dry season, resulting in a generally decrease in monsoon seasonality index (MSI) (see Materials and Methods; fig. S5), although MSI slightly increased when southern Tibet rose comparing to the Gangdese mountains uplifted simulation. Temperatures altered very little in eastern Asia as northern Tibet rose (fig. S6), so compared to precipitation, temperature seems contribute very little to vegetation and plant diversity change. The above analysis indicates that, although summer precipitation changes may have contributed somewhat, winter precipitation increase was the most important factor in determining substantial changes in vegetation and plant diversity in eastern Asia.

In some parts of the north Indochina Peninsula (10°N to 20°N), the simulated results show dry winter precipitation (Fig. 3, A1 to A4) but evergreen broadleaf forests (Fig. 2, B1 to B4), especially in the northwest region around the Sundarbans delta. This region indicates higher soil moisture in deep layers (40 to 200 cm) for both low and high Tibetan experiments, even in the dry season, compared to southeast Asia with similar dry winter conditions (fig. S7). The low elevation of this delta generally means saturated soils year round. Because deep soil moisture is vital for evergreen forest transpiration during the dry season in tropical monsoon Asia, it is an important process imbedded in SDGVM (*27*); therefore, the simulated evergreen broadleaf forest was promoted because of high deep soil moisture predicted in the climate simulations. Other factors such as vapor pressure deficit and relative humid conditions could also have contributed to the difference of simulated vegetation types under the similar precipitation conditions.

The critical role of winter precipitation for determining subtropical vegetation in eastern Asia is further supported by physiological and paleobotanical studies (*33*, *34*). Most of the evergreen broadleaf species produce desiccation-sensitive (recalcitrant) seeds (*33*). Many of these species cannot survive a severe/prolonged dry season (*33*). For example, most species of evergreen oak (*Quercus* section *Cyclobalanopsis*), a dominant component in tropical and subtropical Asia, produce desiccation-sensitive seeds (*34*). Precipitation during the dry season

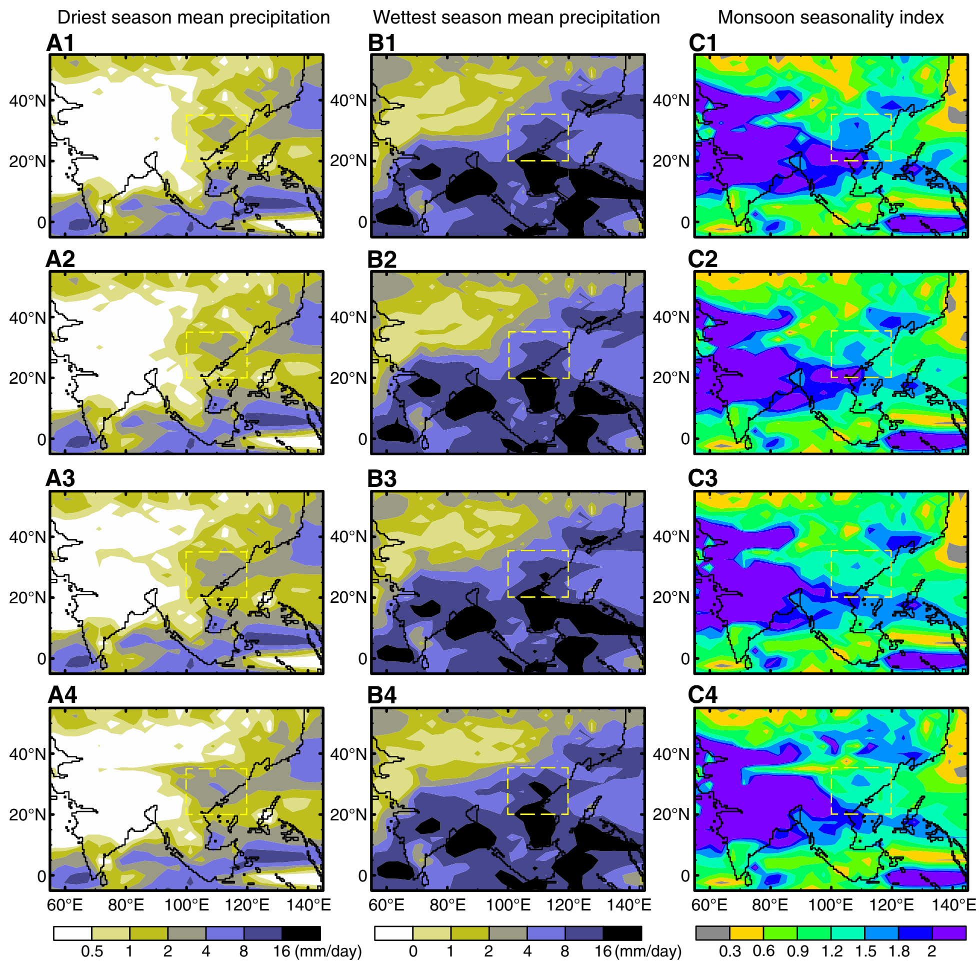

Fig. 3. Simulated precipitation results from selected four experiments with different Tibetan Plateau topographies. Panels (**A1**) to (**A4**), (**B1**) to (**B4**), and (**C1**) to (**C4**) show driest season (DJF), wettest season (JJA) precipitation, and monsoon seasonality index (see Materials and Methods for the definition) for different experiments, respectively. The yellow color dashed boxes indicate the East Asia region (100°E to 120°E, 20°N to 35°N) discussed in the main text. See Supplementary Text for more details for the selection of four simulations.

thus plays a critical role in determining the distribution of these desiccation sensitive taxa. The fossil floral data also indicate a large region of south China was exceptionally warm and humid in winter during the Miocene (*5*). This provided a favorable climate for evergreen broadleaf forests and, leading their expansion during the Miocene.

The mechanism that increased winter precipitation is a relatively simple one in which the East Asia winter monsoon winds (the eastward and southward cold air flows caused by Siberia-Mongolia high-pressure systems) were deflected by the topography of northern Tibet (Fig. 4). Mean sea level pressure decreased significantly over the northwest of China (fig. S8) as northern Tibet rose, allowing the southerly winds to invade the northern part of eastern Asia (fig. S9, A, C, and E). Meanwhile, the vertical velocity (mean value of 80°E to 110°E) in winter around latitudes of ~30°N changed from positive to negative values as northern Tibet rose, indicating that ascending air can reach to higher levels in the atmosphere (around 250 hPa; fig. S10, A and C). The convergent flows and upward movement can, therefore, substantially enhance moisture supply in winter. When Tibet rose, summer southeasterly winds increased over southeastern Asia (fig. S9, B, D, and F), and the vertical velocity decreased relatively around 20°N to 35°N (fig. S10, B and D), implying that the intertropical convergence zone moved further north. This intensifies the summer monsoon due to the strengthening of the differential heating of land and ocean produced by high topography in the Tibetan region (*35*). These effects thus generated relatively strong ascending air, increasing summer rainfall in this region.

The vast majority of previous modeling studies have focused on sensitivity tests associated with present day geographies, and this may lead to a misleading interpretation for past changes. This is because we have shown that the mechanism is related to the interaction between Tibet and the circulation, and both are potentially shifted in latitude compared to the modern. Even a small change in latitude could shift patterns, and hence, modern sensitivity tests may have limited value for interpreting past changes. Existing modeling has shown that a unitary rise of Tibet generally brings wetter summers to southeast Asia due to an intensified summer monsoon (*9*–*11*, *14*, *15*, *36*), although most modeling works mainly focus on drying trends in the Asian interior (*10*, *14*, *18*, *36*). However, these kinds of simulations have produced variable results with regard to the winter monsoon. An earlier atmospheric GCM experiment produced a winter monsoon over eastern Asia as a unitary Tibet rose, but winter precipitation changed very little in southeastern China (*36*). An *et al.* (*10*) showed that the growth of the northern and eastern margins of Tibet enhanced winter monsoon rains in East Asia and produced a dry climate in central Asia, but there was no evidence of

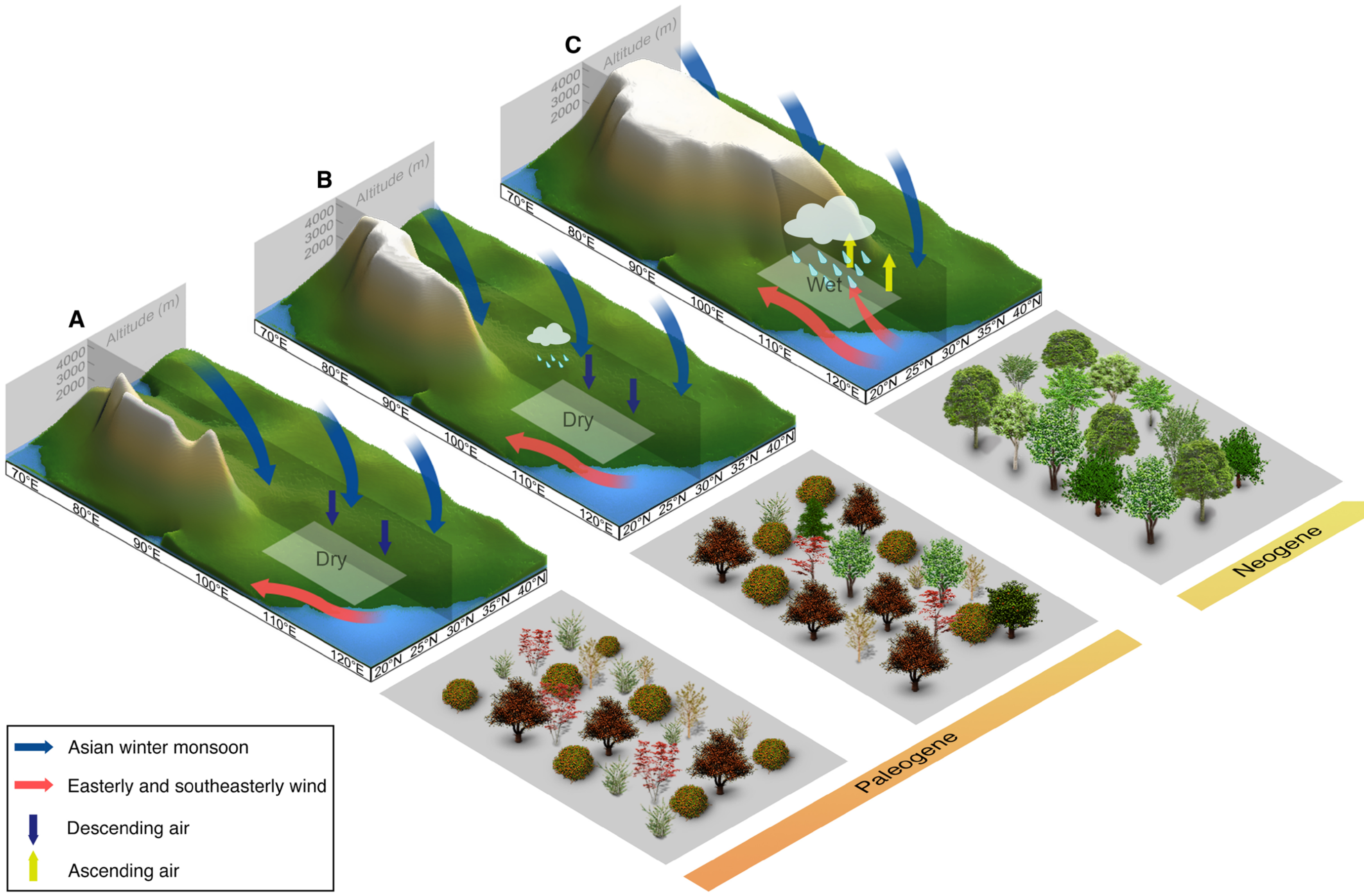

Fig. 4. Simplified Tibet uplift stages, climate, and vegetation changes from the Paleogene to Neogene. (**A** and **B**) When the Gangdese Mountains and Lhasa Terrane uplifted, respectively, the strong Asian winter monsoon caused dry climate, producing deciduous broadleaf forest and shrub in eastern Asia. (**C**) When the Qiangtang and Songpan-Ganzi terranes uplifted, the weak Asian winter monsoon and invaded southeasterly winds enhanced winter precipitations, resulting in evergreen broadleaf forest in southeastern Asia. The topographies of (A) to (C) are modified from Fig. 2 (A1, A2, and A4, respectively).

change in southeastern China. Zhang *et al.* (*18*) conducted eight experiments based on modern, not paleo-, geography using the National Center for Atmospheric Research Community Atmosphere Model (Community Atmosphere Model 4). The results indicated rises of central-southern and northern Tibet increased the Siberian High and thus enhanced East Asian winter monsoon, causing drier winters in eastern Asia.

While this result conflicts with our findings, other modeling experiments support our results. Kutzbach *et al.* (*14*) conducted sensitivity experiments with three different Tibetan Plateau topographies using the Community Climate Model, showing winter precipitation increased to the south and east of the plateau when the Tibet was elevated (*14*). In different experiments, the same model produced wetter winters along the east Asian coast when there was plateau uplift in southern Asia and the American West (*37*). Recently, Sha *et al.* (*38*) applied the same model as Zhang *et al.* (*18*) but at higher resolution. Their results demonstrated that, with an elevated Tibet, East Asian winter monsoon increased in northern China but decreased in southeastern China, inducing substantial winter precipitation increase over southeastern Asia (*38*). Zoura *et al.* (*17*) also showed winter monsoon changes similar to our results, although they use a very similar model. The notable strengthening of the southerly winds and increasing of precipitation in dry season in southeastern China is consistent with our results. The disparities between models need to be explored in future works but using real paleogeographies rather than interpreting present day sensitivity tests.

It is not just the elevation of Tibet that influences Asian climate. Other orographic highs to the north and west of present Tibetan Plateau, such as the Tian Shan Mountains, the Pamir Plateau, and the Mongolia Plateau experienced substantial topographic change during the Cenozoic (*39*–*42*). These topographic changes could exert prominent climate effects on eastern Asia. A recent sensitivity experiment indicated that when the Tian Shan Mountains and the Pamir Plateau were elevated, the East Asian winter monsoon intensified (*38*). There was obvious strengthening of northerly winds and reduction of precipitation in northeastern China, but southern China showed little change (*38*). A rise of Mongolia slightly increased the winter monsoon, but the vertical velocities changed little in southeastern China (*43*). Overall, uplift of the Tian Shan mountains, the Pamir Plateau, and the Mongolia Plateau can intensify the East Asian winter monsoon in northeastern Asia, but the climate effects across southeastern Asia are weak. These topographic changes cannot, therefore, be the main factor driving the increase in winter precipitation in southeastern China (*38*, *43*–*45*).

Our results imply that the topographic growth in northern Tibet has greater vegetation and plant diversity impacts than rises in the south. Any rise of the north and northeastern parts of Tibet causes a weakening of the winter monsoon, resulting in much more prominent increased winter precipitation over eastern Asia, a sharp transition to a more humid climate, major changes in vegetation patterns, and an increase in plant diversity (Fig. 4). These changes are seen in fossil records near the end of the Paleogene. We infer that, although southern Tibet was already high long before the Oligocene, the rise of northern and eastern Tibet was ongoing throughout the Paleogene-Neogene transition as evidenced by recent fossil data (*22*, *46*–*48*), and there is a strong case for revisiting existing stable isotope paleoaltimetry due to the complexity of fractionation that must have resulted from air parcel trajectory changes during the piecemeal growth of Tibet (*13*, *49*). Our research highlights that, when using climate models to evaluate proxy data and the history of Tibet, it is important to use realistic representations of the complex Tibetan orographic history and not treat Tibet as a simple monolithic plateau.

MATERIALS AND METHODS

Cenozoic vegetation maps of China

We reconstruct two different Cenozoic vegetation maps based on paleobotanical data in China. The first reconstructed vegetation map (fig. S1) is derived from the primary literatures and reported fossil taxa, interpreted according to the SDGVM criteria (*26*). For instance, the deciduous broadleaf and shrub, deciduous broadleaf mixed with conifers, deciduous broadleaf mixed with evergreen broadleaf, etc., are mainly composed of deciduous broadleaf taxa. In most cases, we assign these floras to deciduous broadleaf types. However, the evergreen broadleaf taxa mixed with deciduous broadleaf taxa, evergreen broadleaf mixed with deciduous broadleaf and shrub taxa, evergreen broadleaf mixed with shrub and grass taxa, etc., normally indicate a large portion of evergreen broadleaf taxa in the floras. In these cases, we assign these floras to evergreen broadleaf dominated floras.

The second reconstructed map shows the boundaries between arid and humid conditions. The arid, semi-arid, humid, and semi-humid vegetation types are derived from the primary literatures based on the fossil taxa as interpreted by Sun and Wang (*5*) and sedimentation data. These interpretations are well respected. For instance, if *Ephedripites* pollen grains exceed 15%, then the palynological assemblage may indicate arid or semiarid environments. Other taxa—such as *Nitraria*, *Artemisia*, Asteraceae, Chenopodiaceae, Poaceae, Zygophyllaceae, etc.—generally imply open vegetation and a dry climate (*5*). The presence of megafossils, such as leaves, representing *Palibinia* also always indicates arid and semiarid climates (*5*). Therefore, we can assign the vegetation types according to these xerophytic plants in fossil floras.

HadAM3 experiments

The UK Hadley Centre Climate Model [HadAM3B-M2.1aD, using the nomenclature of Valdes *et al.* (*24*)] is used for these paleogeographic sensitivity simulations. The model resolution is 3.75° × 2.5° for longitude and latitude and 19 levels in the vertical. We conduct 18 paleogeography sensitivity experiments to investigate the detailed role of Tibetan orogeny on climate using the control run. The SSTs, topography, geography, and land-sea boundary conditions are prescribed as in previous Chattian simulations (*50*). All the simulations are run for 100 years and reached equilibrium. The last 30 years of simulated data are extracted for climate analysis and vegetation/biodiversity simulations. The prescribed partial pressure of CO_2 (PCO_2) for all the simulations is 560 parts per million by volume (ppmv) (*51*).

Although ocean-atmosphere–coupled GCM models can fully explore ocean and atmosphere feedbacks, the uncoupled model tests large-scale climate affected by different topographies. A previous work using a general circulation model (UK Met Office GCM, HadCM3L) (*19*) has shown that Tibetan uplift had relatively minor impacts on the SSTs in the South China Sea, western Pacific, and Indian Ocean; thus, the ocean circulation caused by topographic changes can be excluded in the simulations, which allows us to focus on the effects of Tibetan orographic development. Other factors such as the Paratethys Sea retreat, the land-sea boundary changes, vegetation dynamics, and CO_2 concentration changes are not evaluated here. The Chattian geography, topography, and ice sheets are derived from the Getech Group plc Paleogeographies collected from numerous geologic studies (*25*).

Topographic boundary conditions

We conduct 18 sensitive experiments on different Tibet uplift topographies from the late Paleogene to early Neogene based on recent geological and fossil data (fig. S3 and data S2) (*12*, *13*, *21*–*23*, *52*, *53*). Several theories have been proposed to explain Tibetan Plateau development history including: (i) the whole "soft Tibet" markedly rose above its present altitude (*30*, *54*, *55*), (ii) outward growth from a higher proto-Tibetan upland (*23*, *56*, *57*) or existence of an east-west trending Tibetan central valley system (*22*), and (iii) Tibetan uplift progressed stepwise northeastward (*12*, *52*, *53*). Although there is still debate about the orographic history of Tibet, most of the recent studies agree that Tibetan terranes separated by the suture zones from north to south were uplifted asynchronously. The core of Tibet including the Lhasa, Qiangtang, and Songpan-Ganzi terranes likely uplifted early during the Paleogene and early Neogene. Other parts of Tibet and surrounding regions including the Himalaya, Kunlun-Qaidam basin, and the Qilian Mountains likely uplifted during the late Neogene (*12*, *52*, *53*, *58*). The Gangdese Mountains reached an elevation of 4500 m in the Paleocene-Eocene (*21*); therefore, we also consider high elevation of the Gangdese Mountains, to explore the impacts of high Gangdese Mountains on climate and vegetation/biodiversity.

We change the Tibetan region (71.25°E to 105°E, 20°N to 40°N) to different topographies based on a Chattian orography (provided by Getech Group plc) (*25*). We set up different Tibetan Plateau regions based on constituent Tibetan terranes (*3*, *12*, *13*, *21*–*23*). To reconstruct roughly comparable range of different Tibetan regions for the late Oligocene and present, the locations of different terranes are transferred to the Chattian paleogeographic framework based on the modern coordinates using the Getech Group plc plate model (*25*). The site 160 (see data S1) is regarded as from the India Plate in the Getech Group plc plate model, so we correct the paleocoordinates of this site using the gplates model (http://portal.gplates.org).

The SDGVM

The SDGVM is used to assess relative importance of climate (e.g., temperature and precipitation) with forcings derived from different model simulations and predicts plant functional types (*26*). The input variables for the SDGVM including monthly temperature, precipitation, relative humidity, cloudiness data, and prescribed soil texture are derived from 18 sensitivity simulations. Seven plant functional types are designed in the SDGVM model, including barren (bare ground or desert), C3 grasses and shrubs, C4 grassland, evergreen broadleaf trees, evergreen needleleaf trees, deciduous broadleaf trees, and deciduous needleleaf trees (*26*).

The JeDi-DGVM

The JeDi-DGVM is a recently developed plant traits-based vegetation/plant diversity model (*27*). The plant diversity can be represented by simulated functional richness, which is defined as the value of surviving growth strategies in a simulated grid divided by the maximum value of surviving growth strategies in simulated grids (*27*). The input variables (derived from four selected simulations) include unit plant available water capacity, temperature, net longwave radiation at the surface, downward shortwave radiation at the surface, and daily total precipitation (*27*).

Validation of the SDGVM and JeDi-DGVM

We simulate the SDGVM and JeDi-DGVM results based on preindustrial conditions using a coupled atmosphere-ocean general circulation model [HadCM3, using the nomenclature of Valdes *et al.* (*24*); see the details in data S2]. We compare the simulated results with modern vegetation derived from terrestrial ecoregions of the world (*59*) and native vascular plant diversity derived from Ellis *et al.* (*60*). The results show the simulated SDGVM is generally consistent with the observed SDGVM in Asia (fig. S11). The south part of eastern Asia is mainly covered by evergreen broadleaf forest, while the north part is covered by deciduous broadleaf forest. The evergreen broadleaf forests in the south Himalaya Mountains are not presented by the model, which could be due to the low resolution of the model, which cannot detect the steep topography of this narrow range. The simulated evergreen broadleaf area in the preindustrial simulation (fig. S11B) in eastern Asia is smaller than that in the experiments with high plateau (fig. S4, E, F, H, I, and O to R). This could be due to the very different boundary conditions between the late Oligocene and present. The prescribed PCO_2 for the late Oligocene simulations is 560 ppmv, while for the preindustrial, it is 280 ppmv (data S2). The low CO_2 simulations could result in low temperature and precipitation in southeastern Asia (*11*), consequently, reduce distribution of the evergreen broadleaf forest in this region. Other factors such as the relative positions of the continents, oceanic ridges, and mountains and the condition of ice sheets are also very different. These differences can fundamentally perturb the atmosphere and ocean circulation, and thus global energy fluxes, which may produce very different climate and vegetation results in East Asia.

To make a clearer comparison, we normalize both modern plant diversity and simulated plant diversity to [0 to 1] by dividing the maximum plant diversity value, respectively. The simulated plant functional diversity of preindustrial conditions basically agrees with the observed data (fig. S12). Both modeling results and observed data show increasing trend of plant diversity from north to south of Asia, although there is a difference in some regions. Pavlick *et al.* (*27*) point that the simulated functional richness is significantly (R^2 = 0.71) correlated with observed plant species richness, confirming that the JeDi-DGVM simulated plant diversity is reliable. In southeastern Asia and northern Asia, the observed plant diversity is lower than the simulated one, which may be because the highest value in the observed one is particularly high in other regions, resulting a relatively low scaled value in these regions. In the south Himalaya Mountains and India peninsula, the simulated result and observed data are not matched well that may be due to the low resolution of the model.

The monsoon seasonality index

The MSI is defined as the difference between local summer and local winter precipitation (i.e., JJA minus DJF precipitation in the northern hemisphere and DJF minus JJA in the southern hemisphere).

SUPPLEMENTARY MATERIALS

Supplementary material for this article is available at http://advances.sciencemag.org/cgi/content/full/7/5/eabc7741/DC1

REFERENCES AND NOTES

1. C. Hoorn, F. P. Wesselingh, H. ter Steege, M. A. Bermudez, A. Mora, J. Sevink, I. Sanmartín, A. Sanchez-Meseguer, C. L. Anderson, J. P. Figueiredo, C. Jaramillo, D. Riff, F. R. Negri, H. Hooghiemstra, J. Lundberg, T. Stadler, T. Särkinen, A. Antonelli, Amazonia through time: Andean uplift, climate change, landscape evolution, and biodiversity. *Science* **330**, 927–931 (2010).
2. G. Dupont-Nivet, W. Krijgsman, C. G. Langereis, H. A. Abels, S. Dai, X. Fang, Tibetan plateau aridification linked to global cooling at the Eocene–Oligocene transition. *Nature* **445**, 635–638 (2007).
3. R. A. Spicer, Tibet, the Himalaya, Asian monsoons and biodiversity–In what ways are they related? *Plant Divers.* **39**, 233–244 (2017).
4. N. Myers, R. A. Mittermeier, C. G. Mittermeier, G. A. B. da Fonseca, J. Kent, Biodiversity hotspots for conservation priorities. *Nature* **403**, 853–858 (2000).
5. X. Sun, P. Wang, How old is the Asian monsoon system?—Palaeobotanical records from China. *Palaeogeogr. Palaeoclimatol. Palaeoecol.* **222**, 181–222 (2005).
6. Z. T. Guo, B. Sun, Z. S. Zhang, S. Z. Peng, G. Q. Xiao, J. Y. Ge, Q. Z. Hao, Y. S. Qiao, M. Y. Liang, J. F. Liu, Q. Z. Yin, J. J. Wei, A major reorganization of Asian climate by the early Miocene. *Clim. Past* **4**, 153–174 (2008).
7. Y.-S. Chen, T. Deng, Z. Zhou, H. Sun, Is the East Asian flora ancient or not? *Natl. Sci. Rev.* **5**, 920–932 (2018).
8. L.-M. Lu, L.-F. Mao, T. Yang, J.-F. Ye, B. Liu, H.-L. Li, M. Sun, J. T. Miller, S. Mathews, H.-H. Hu, Y.-T. Niu, D.-X. Peng, Y.-H. Chen, S. A. Smith, M. Chen, K.-L. Xiang, C.-T. Le, V.-C. Dang, A.-M. Lu, P. S. Soltis, D. E. Soltis, J.-H. Li, Z.-D. Chen, Evolutionary history of the angiosperm flora of China. *Nature* **554**, 234–238 (2018).
9. D. G. Hahn, S. Manabe, The role of mountains in the south Asian monsoon circulation. *J. Atmos. Sci.* **32**, 1515–1541 (1975).
10. A. Zhisheng, J. E. Kutzbach, W. L. Prell, S. C. Porter, Evolution of Asian monsoons and phased uplift of the Himalaya–Tibetan plateau since Late Miocene times. *Nature* **411**, 62–66 (2001).
11. A. Farnsworth, D. J. Lunt, S. A. Robinson, P. J. Valdes, W. H. G. Roberts, P. D. Clift, P. Markwick, T. Su, N. Wrobel, F. Bragg, S.-J. Kelland, R. D. Pancost, Past East Asian monsoon evolution controlled by paleogeography, not CO_2. *Sci. Adv.* **5**, eaax1697 (2019).
12. P. Tapponnier, X. Zhiqin, F. Roger, B. Meyer, N. Arnaud, G. Wittlinger, Y. Jingsui, Oblique stepwise rise and growth of the Tibet Plateau. *Science* **294**, 1671–1677 (2001).
13. R. A. Spicer, T. Su, P. J. Valdes, A. Farnsworth, F.-X. Wu, G. Shi, T. E. V. Spicer, Z. Zhou, Why 'the uplift of the Tibetan Plateau' is a myth? *Natl. Sci. Rev.* , nwaa091 (2020).
14. J. E. Kutzbach, W. L. Prell, W. F. Ruddiman, Sensitivity of Eurasian climate to surface uplift of the Tibetan Plateau. *J. Geol.* **101**, 177–190 (1993).
15. F. Fluteau, G. Ramstein, J. Besse, Simulating the evolution of the Asian and African monsoons during the past 30 Myr using an atmospheric general circulation model. *J. Geophys. Res.* **104**, 11995–12018 (1999).
16. W. R. Boos, Z. Kuang, Dominant control of the South Asian monsoon by orographic insulation versus plateau heating. *Nature* **463**, 218–222 (2010).
17. D. Zoura, D. J. Hill, A. M. Dolan, S. J. Hunter, Z. Tang, A. M. Haywood, Atmospheric carbon dioxide, ice sheet and topographic constraints on palaeo moisture availability in Asia. *Earth Planet. Sci. Lett.* **519**, 12–27 (2019).
18. R. Zhang, D. Jiang, Z. Zhang, E. Yu, The impact of regional uplift of the Tibetan Plateau on the Asian monsoon climate. *Palaeogeogr. Palaeoclimatol. Palaeoecol.* **417**, 137–150 (2015).
19. D. J. Lunt, R. Flecker, P. D. Clift, The impacts of Tibetan uplift on palaeoclimate proxies. *Geol. Soc. Lond. Spec. Publ.* **342**, 279–291 (2010).
20. R. Zhang, D. Jiang, Z. Zhang, Vegetation and ocean feedbacks on the Asian climate response to the uplift of the Tibetan Plateau. *J. Geophys. Res. Atmos.* **124**, 6327–6341 (2019).
21. L. Ding, Q. Xu, Y. Yue, H. Wang, F. Cai, S. Li, The Andean-type Gangdese Mountains: Paleoelevation record from the Paleocene–Eocene Linzhou Basin. *Earth Planet. Sci. Lett.* **392**, 250–264 (2014).
22. T. Su, A. Farnsworth, R. A. Spicer, J. Huang, F.-X. Wu, J. Liu, S.-F. Li, Y.-W. Xing, Y.-J. Huang, W.-Y.-D. Deng, H. Tang, C.-L. Xu, F. Zhao, G. Srivastava, P. J. Valdes, T. Deng, Z.-K. Zhou, No high Tibetan Plateau until the Neogene. *Sci. Adv.* **5**, eaav2189 (2019).
23. C. Wang, X. Zhao, Z. Liu, P. C. Lippert, S. A. Graham, R. S. Coe, H. Yi, L. Zhu, S. Liu, Y. Li, Constraints on the early uplift history of the Tibetan Plateau. *Proc. Natl. Acad. Sci. U.S.A.* **105**, 4987–4992 (2008).
24. P. J. Valdes, E. Armstrong, M. P. S. Badger, C. D. Bradshaw, F. Bragg, M. Crucifix, T. Davies-Barnard, J. J. Day, A. Farnsworth, C. Gordon, P. O. Hopcroft, A. T. Kennedy, N. S. Lord, D. J. Lunt, A. Marzocchi, L. M. Parry, V. Pope, W. H. G. Roberts, E. J. Stone, G. J. L. Tourte, J. H. T. Williams, The BRIDGE HadCM3 family of climate models: HadCM3@Bristol v1.0. *Geosci. Model Dev.* **10**, 3715–3743 (2017).
25. D. J. Lunt, A. Farnsworth, C. Loptson, G. L. Foster, P. Markwick, C. L. O'Brien, R. D. Pancost, S. A. Robinson, N. Wrobel, Palaeogeographic controls on climate and proxy interpretation. *Clim. Past* **12**, 1181–1198 (2016).
26. F. I. Woodward, M. R. Lomas, Vegetation dynamics-simulating responses to climatic change. *Biol. Rev.* **79**, 643–670 (2004).
27. R. Pavlick, D. T. Drewry, K. Bohn, B. Reu, A. Kleidon, The Jena Diversity-Dynamic Global Vegetation Model (JeDi-DGVM): A diverse approach to representing terrestrial biogeography and biogeochemistry based on plant functional trade-offs. *Biogeosciences* **10**, 4137–4177 (2013).
28. H.-Y. Hou, Vegetation of China with reference to its geographical distribution. *Ann. Missouri Bot. Gard.* **70**, 509–549 (1983).
29. X.-Q. Yu, L.-M. Gao, D. E. Soltis, P. S. Soltis, J.-B. Yang, L. Fang, S.-X. Yang, D.-Z. Li, Insights into the historical assembly of East Asian subtropical evergreen broadleaved forests revealed by the temporal history of the tea family. *New Phytol.* **215**, 1235–1248 (2017).
30. P. England, G. Houseman, Extension during continental convergence, with application to the Tibetan Plateau. *J. Geophys. Res. Solid Earth* **94**, 17561–17579 (1989).
31. T. M. Harrison, P. Copeland, W. S. F. Kidd, A. Yin, Raising Tibet. *Science* **255**, 1663–1670 (1992).
32. U. Linnemann, T. Su, L. Kunzmann, R. A. Spicer, W.-N. Ding, T. E. V. Spicer, J. Zieger, M. Hofmann, K. Moraweck, A. Gärtner, A. Gerdes, L. Marko, S.-T. Zhang, S.-F. Li, H. Tang, J. Huang, A. Mulch, V. Mosbrugger, Z.-K. Zhou, New U-Pb dates show a Paleogene origin for the modern Asian biodiversity hot spots. *Geology* **46**, 3–6 (2018).
33. J. C. Tweddle, J. B. Dickie, C. C. Baskin, J. M. Baskin, Ecological aspects of seed desiccation sensitivity. *J. Ecol.* **91**, 294–304 (2003).
34. K. Xia, M. I. Daws, F. R. Hay, W.-Y. Chen, Z.-K. Zhou, H. W. Pritchard, A comparative study of desiccation responses of seeds of Asian Evergreen Oaks, *Quercus* subgenus *Cyclobalanopsis* and *Quercus* subgenus *Quercus*. *South Afr. J. Bot.* **78**, 47–54 (2012).
35. H. A. Armstrong, M. B. Allen, Shifts in the intertropical convergence zone, Himalayan exhumation, and late Cenozoic climate. *Geology* **39**, 11–14 (2011).
36. X. Liu, Z.-Y. Yin, Sensitivity of East Asian monsoon climate to the uplift of the Tibetan Plateau. *Palaeogeogr. Palaeoclimatol. Palaeoecol.* **183**, 223–245 (2002).
37. W. F. Ruddiman, J. E. Kutzbach, Forcing of late Cenozoic northern hemisphere climate by plateau uplift in southern Asia and the American West. *J. Geophys. Res.* **94**, 18409–18427 (1989).
38. Y. Sha, Z. Shi, X. Liu, Z. An, X. Li, H. Chang, Role of the Tian Shan Mountains and Pamir Plateau in increasing spatiotemporal differentiation of precipitation over interior Asia. *J. Climate* **31**, 8141–8162 (2018).
39. A. Hellwig, S. Voigt, A. Mulch, K. Frisch, A. Bartenstein, J. Pross, A. Gerdes, T. Voigt, Late Oligocene to early Miocene humidity change recorded in terrestrial sequences in the Ili Basin (south-eastern Kazakhstan, Central Asia). *Sedimentology* **65**, 517–539 (2018).
40. J. K. Caves, B. U. Bayshashov, A. Zhamangara, A. J. Ritch, D. E. Ibarra, D. J. Sjostrom, H. T. Mix, M. J. Winnick, C. P. Chamberlain, Late Miocene uplift of the Tian Shan and Altai and reorganization of Central Asia climate. *GSA Today* **27**, 19–26 (2017).
41. J. K. Caves, D. J. Sjostrom, H. T. Mix, M. J. Winnick, C. P. Chamberlain, Aridification of Central Asia and uplift of the Altai and Hangay Mountains, Mongolia: Stable isotope evidence. *Am. J. Sci.* **314**, 1171–1201 (2014).
42. X. Wang, D. Sun, F. Chen, F. Wang, B. Li, S. V. Popov, S. Wu, Y. Zhang, Z. Li, Cenozoic paleo-environmental evolution of the Pamir–Tien Shan convergence zone. *J. Asian Earth Sci.* **80**, 84–100 (2014).
43. Z. Shi, X. Liu, Y. Liu, Y. Sha, T. Xu, Impact of Mongolian Plateau versus Tibetan Plateau on the westerly jet over North Pacific Ocean. *Climate Dynam.* **44**, 3067–3076 (2015).
44. R. Zhang, D. Jiang, Z. Zhang, Z. G. Cheng, Q. Zhang, Comparison of the climate effects of surface uplifts from the northern Tibetan Plateau, the Tianshan, and the Mongolian Plateau on the East Asian climate. *J. Geophys. Res. Atmos.* **122**, 7949–7970 (2017).
45. X. Wang, B. Carrapa, Y. Sun, D. L. Dettman, J. B. Chapman, J. K. Caves Rugenstein, M. T. Clementz, P. G. DeCelles, M. Wang, J. Chen, J. Quade, F. Wang, Z. Li, I. Oimuhammadzoda, M. Gadoev, G. Lohmann, X. Zhang, F. Chen, The role of the westerlies and orography in Asian hydroclimate since the late Oligocene. *Geology* **48**, 728–732 (2020).
46. B. Song, R. A. Spicer, K. Zhang, J. Ji, A. Farnsworth, A. C. Hughes, Y. Yang, F. Han, Y. Xu, T. Spicer, T. Shen, D. J. Lunt, G. Shi, Qaidam Basin leaf fossils show northeastern Tibet was high, wet and cool in the early Oligocene. *Earth Planet. Sci. Lett.* **537**, 116175 (2020).
47. T. Su, R. A. Spicer, S.-H. Li, H. Xu, J. Huang, S. Sherlock, Y.-J. Huang, S.-F. Li, L. Wang, L.-B. Jia, W.-Y.-D. Deng, J. Liu, C.-L. Deng, S.-T. Zhang, P. J. Valdes, Z.-K. Zhou, Uplift, climate and biotic changes at the Eocene–Oligocene transition in south-eastern Tibet. *Natl. Sci. Rev.* **6**, 495–504 (2018).
48. T. Deng, X. Wang, F. Wu, Y. Wang, Q. Li, S. Wang, S. Hou, Implications of vertebrate fossils for paleo-elevations of the Tibetan Plateau. *Glob. Planet. Change* **174**, 58–69 (2019).
49. P. J. Valdes, D. Lin, A. Farnsworth, R. A. Spicer, S.-H. Li, T. Su, Comment on "Revised paleoaltimetry data show low Tibetan Plateau elevation during the Eocene". *Science* **365**, eaax8474 (2019).
50. S. Li, Y. Xing, P. J. Valdes, Y. Huang, T. Su, A. Farnsworth, D. J. Lunt, H. Tang, A. T. Kennedy, Z. Zhou, Oligocene climate signals and forcings in Eurasia revealed by plant macrofossil and modelling results. *Gondw. Res.* **61**, 115–127 (2018).
51. D. J. Beerling, D. L. Royer, Convergent Cenozoic CO_2 history. *Nat. Geosci.* **4**, 418–420 (2011).

52. X. Liu, Q. Xu, L. Ding, Differential surface uplift: Cenozoic paleoelevation history of the Tibetan Plateau. *Sci. China Earth Sci.* **59**, 2105–2120 (2016).
53. L. H. Royden, B. C. Burchfiel, R. D. van der Hilst, The geological evolution of the Tibetan Plateau. *Science* **321**, 1054–1058 (2008).
54. P. Molnar, P. England, J. Martinod, Mantle dynamics, uplift of the Tibetan Plateau, and the Indian monsoon. *Rev. Geophys.* **31**, 357–396 (1993).
55. J. P. Platt, P. C. England, Convective removal of lithosphere beneath mountain belts: Thermal and mechanical consequences. *Am. J. Sci.* **293**, 307–336 (1993).
56. J. P. Burg, G. M. Chen, Tectonics and structural zonation of southern Tibet, China. *Nature* **311**, 219–223 (1984).
57. J. F. Dewey, S. Cande, W. C. Pitman, The tectonic evolution of the India/Eurasia collision zone. *Eclogae Geol. Helv*. **82**, 717–734 (1989).
58. P. J. Polissar, K. H. Freeman, D. B. Rowley, F. A. McInerney, B. S. Currie, Paleoaltimetry of the Tibetan Plateau from D/H ratios of lipid biomarkers. *Earth Planet. Sci. Lett*. **287**, 64–76 (2009).
59. D. M. Olson, E. Dinerstein, E. D. Wikramanayake, N. D. Burgess, G. V. N. Powell, E. C. Underwood, J. A. D'amico, I. Itoua, H. E. Strand, J. C. Morrison, C. J. Loucks, T. F. Allnutt, T. H. Ricketts, Y. Kura, J. F. Lamoreux, W. W. Wettengel, P. Hedao, K. R. Kassem, Terrestrial ecoregions of the world: A new map of life on earth: A new global map of terrestrial ecoregions provides an innovative tool for conserving biodiversity. *Bioscience* **51**, 933–938 (2001).
60. E. C. Ellis, E. C. Antill, H. Kreft, All is not loss: Plant biodiversity in the Anthropocene. *PLOS ONE* **7**, e30535 (2012).
61. Q. Xu, L. Ding, L. Zhang, F. L. Cai, Q. Lai, D. Yang, J. Liu-Zeng, Paleogene high elevations in the Qiangtang Terrane, central Tibetan Plateau. *Earth Planet. Sci. Lett*. **362**, 31–42 (2013).
62. Y. Miao, F. Wu, H. Chang, X. Fang, T. Deng, J. Sun, C. Jin, A Late-Eocene palynological record from the Hoh Xil Basin, northern Tibetan Plateau, and its implications for stratigraphic age, paleoclimate and paleoelevation. *Gondw. Res.* **31**, 241–252 (2016).
63. Q. Xu, X. Liu, L. Ding, Miocene high-elevation landscape of the eastern Tibetan Plateau. *Geochem. Geophys. Geosyst.* **17**, 4254–4267 (2016).
64. D. W. Burbank, Causes of recent Himalayan uplift deduced from deposited patterns in the Ganges basin. *Nature* **357**, 680–683 (1992).
65. X. Z. Xiong, Palaeocene flora from the Wuyun Formation in Jiayin of Heilongjiang. *Acta Palaeontol. Sin.* **25**, 571–576 (1986).
66. M.-L. Liu, The late Upper Cretaceous to Palaeocene sporopollen assemblages from the Furao area, Heilongjiang Province. *Bull. Shenyang Inst. Geol. Miner. Resour. Chin. Acad. Geol. Sci.* **7**, 99–132 (1983).
67. Y. Zhang, P. M. Zhai, S. L. Zheng, W. Zhang, Late Cretaceous–Paleogene plants from Tangyuan, Heilongjiang. *Acta Palaeontol. Sin.* **29**, 237–245 (1990).
68. C. B. Zhao, D. Ye, B. Chen, D. Liu, in *Tertiary in Petroliferous Regions of China, III. The Northeast Region of China* (Petroleum Industry Press, 1994), pp. 1–156.
69. C.-x. He, J.-r. Tao, A study on the Eocene flora in Yilan County, Heilongjiang, China. *J. Syst. Evol.* **35**, 249–256 (1997).
70. M. Liu, N. Q. Du, Z. C. Kong, Palynological analysis of the late Cenozoic and its significance in Fulaerji, Heilongjiang Province. *Acta Bot. Sin.* **32**, 307–316 (1990).
71. G. W. Liu, H. M. Li, Q. Leng, A preliminary report on Miocene flora from Daotaiqiao formation of Huanan County, Heilongjiang Province, NE China. *Acta Palaeontol. Sin.* **34**, 755–757 (1995).
72. S. X. Guo, G. F. Zhang, Oligocene Sanhe flora in Longjing county of Jilin, northeast China. *Acta Palaeontol. Sin.* **41**, 193–210 (2002).
73. Y. Zhang, K. Wang, J. Wang, Pollen assemblages from Hunchun Coalmine of Hunchun, Jilin Province and its paleovegetational and paleoclimatic significance. *Coal Geol. Explor.* **1**, 18–25 (1987).
74. H. M. Li, G. Y. Yang, Miocene Qiuligou flora in Dunhua County Jilin Province. *Acta Palaeontol. Sin.* **2**, (1984).
75. C. H. Jia, L. Yu, N.-Q. Du, Z.-C. Kong, Changes of vegetation and climate in Qian An County, Jilin Province since late Tertiary. *Sci. Geogr. Sin.* **9**, 272–282 (1989).
76. Z. C. Song, L. Tsao, The Paleocene spores and pollen grains from the Fushun coal field, Northeast China. *Acta Palaeontol. Sin.* **15**, 147–164 (1976).
77. J.-r. Li, J.-l. Xu, Y.-m. Yang, Paleocene sporopollen assemblages from northern Shandong. *Acta Palaeontol. Sin.* **31**, 445–458 (1992).
78. J. R. Tao, J. J. Yang, Y. F. Wang, Miocene wood fossils and paleoclimate in inner Monggolia. *Acta Bot. Yunnanica* **16**, 111–116 (1994).
79. Z. B. Gan, Spore-Pollen Assemblage from the Early Miocene of Wuluogong, Northern Hebei, in *Selected Papers from the First Symposium of the Palynological Society of China* (Science Press, 1982), pp. 59–63.
80. L. F. Tong, R. G. Gu, Lower tertiary biota and environment of Huanghua Basin. *Earth Sci. China Univ. Geosci.* **2**, 1–7 (1985).
81. W. Y. Li, Y. L. Liang, The pliocene sporo-pollen assemblage of huanghua in hebei plain and its significance in Palaeobotany and Palaeoecology. *Acta Bot. Sin.* **23**, 478–486 (1981).
82. Y. M. Yao, H. Liang, Z. Cai, X. T. Guan, Z. Q. Zhao, Z. Q. Cheng, Z. C. Sun, S. Z. Yang, in *Tertiary in Petroliferous Regions of China (IV): The Bohai Gulf Basin* (Petroleum Industry Press, 1994), pp. 1–240.
83. M. Tao, K. Wang, G. Zheng, C. Zhi, Early Tertiary sporopollen assemblages from Jizhong depression and their stratigraphic implication. *Acta Micropalaeontologica Sin.* **18**, 274–292 (2001).
84. W. M. Wang, Sporo-pollen assemblage from the Miocene Tongguer Formation of Inner Mongolia and its climate. *Acta Bot. Sin.* **32**, 901–904 (1990).
85. H. M. Li, Q. S. Chen, *Palibinia* from the Eocene of Jiangxi, China—With remarks on the dry climate mechanism of northern hemisphere in paleogene. *Acta Palaeontol. Sin.* **41**, 119–129 (2002).
86. W. M. Wang, D. H. Zhang, Tertiary sporo-pollen assemblages from the Shangdu-Huade Basin, Inner Mongolia: With discussion on the formation of steppe vegetation in China. *Acta Micropalaeontologica Sin.* **7**, 239–252 (1990).
87. X. M. Wang, X. Q. Zhang, M. Z. Wang, C. S. Li, The palynoflora from Paleogene of Fanshi, Shanxi and discussion on their geological age. J. *Shandong Univ. Sci. Technol.* **22**, 26–32 (2003).
88. Z. C. Zhang, Tertiary fossil plants from Pingzhuang of Ju'ud League, Nei Mongol (Inner Mongolia). *Bull. Shenyang Inst. Geol. Miner. Ressources.* **14**, 117–124 (1986).
89. G. Liu, E. B. Leopold, Y. Liu, W. Wang, Z. Yu, G. Tong, Palynological record of Pliocene climate events in North China. *Rev. Palaeobot. Palynol.* **119**, 335–340 (2002).
90. J. R. Tao, Discover of *Palibinia* from Puyang of Henan, and its paleoclimatic significance. *Bull. Bot.* **1**, 50–52 (1983).
91. G. Liu, E. B. Leopold, Climatic comparison of Miocene pollen floras from northern East-China and south-central Alaska, USA. *Palaeogeogr. Palaeoclimatol. Palaeoecol.* **108**, 217–228 (1994).
92. C. X. Tong, X. Q. Zhang, Sporo-pollen assemblages from the Guanzhuang Formation of the lower Tertiary in the Tailai Basin, Shandong and their geological significance. *L. Resour. Shandong Prov.* **4**, 40–50 (1987).
93. Z. C. Song, Y. H. Zheng, J. L. Liu, P. Y. Ye, in *Cretaceous-Tertiary Palynological Assemblages from Jiangsu* (Geological Publishing House, 1981), pp. 1–214.
94. S. B. Zhang, H. Shen, X. Qu, Q. Gao, in *Tertiary in Petroliferous Regions of China. The Hubei–Henan–Anhui Region, Vol. V* (Petroleum Industry Press, 1993), pp. 1–296.
95. H. M. Li, J. J. Shao, J. N. Huang, Some Neogene plant fossils from Nanjing area, Jiangsu. *Acta Palaeontol Sin.* **26**, 563–575 (1987).
96. M. Y. Li, Eocene pollen and spore assemblage from Wuhu. *Acta. Palaeobot. Palynol. Sin.* **1**, 141–161 (1986).
97. H. H. Zhao, S. Y. Guo, in *Stratigraphic Paleontology of Zhoukou and Nanyang Areas, Henan Province* (Geological Publishing House, 1995).
98. D.-N. Wang, X.-Y. Sun, Y.-N. Zhao, The Paleocene-Eocene palynoflora from the Tantou Basin in west Henan. *J. Integr. Plant Biol.* **26**, 448–455 (1984).
99. J. R. Tao, Z. K. Zhou, Y. S. Liu, in *The Evolution of the Late Cretaceous-Cenozoic Floras in China* (Science Press, 2000), pp. 1–282.
100. D. N. Wang, X. Y. Sun, Y. N. Zhao, Z. S. He, Late Cretaceous to Paleogene sporopollen assemblage sequence in some parts of China. *Geol. Rev.* **30**, 8–18 (1984).
101. G. B. Tong, M. P. Zheng, H. R. Yuan, J. Y. Li, Y. C. Li, A study of middle and late Eocene palynological assemblages in Jianghan Basin and their environmental significance. *Acta Geosci. Sin.* **22**, 73–78 (2001).
102. Y. C. Wang, Y. Mu, X. Ju, Z. Ye, Z. Zhao, in *Tertiary in Petroliferous Regions of China, VI. The Southeast Region of China* (Petroleum Industry Press, 1994), pp. 1–246.
103. Y. H. Zheng, Miocene pollen and spores from Xianju–Ninghai, Zhejiang, in *Selected Papers of the 1st Scientific Conference of the Palynological Society of China* (Science Press, 1982), pp. 71–74.
104. F. M. B. Jacques, G. Shi, W. Wang, Reconstruction of Neogene zonal vegetation in South China using the Integrated Plant Record (IPR) analysis. *Palaeogeogr. Palaeoclimatol. Palaeoecol.* **307**, 272–284 (2011).
105. Y. H. Zheng, Fossil pollen grains of Podocarpaceae from Upper Tertiary in Fujian. *Acta Palaeontol. Sin.* **5**, 605–617 (1987).
106. M. Y. Li, Sporo-pollen from Shanghu Formation of Early Paleocene in Nanxiong Basin, Guangdong. *Acta Palaeontol. Sin.* **28**, 741–749 (1989).
107. Z. J. Wu, J. F. Yu, Late Paleocene spores and pollen grains from the uppermost part of Nongshan group in Nanxiong Basin, Guangdong. *Acta Palaeontol Sin.* **20**, 442–448 (1981).
108. M. R. Sun, X. Y. Sun, Y. N. Zhao, D. N. Wang, Z. R. Li, Z. H. Hu, J. R. Xu, P. F. Mei, in *Cenozoic Paleobiota of the Continental Shelf of the East China Sea (Donghai), Micropaleobotanical Volume* (Geological Publishing House, 1989), pp. 6–111.
109. S. X. Guo, Note on Phytogeographic Province and Ecological Environment of Late Cretaceous and Tertiary Floras in China, in *Editorial Committee of Foundamental Theory of Palaeontology book Series in China (Ed.), Palaeobiogeography Provinces of China* (Science Press, 1983), pp. 164–177.
110. F. M. B. Jacques, G. Shi, T. Su, Z. Zhou, A tropical forest of the middle Miocene of Fujian (SE China) reveals Sino-Indian biogeographic affinities. *Rev. Palaeobot. Palynol.* **216**, 76–91 (2015).

111. S. X. Guo, Late Cretaceous and Early Tertiary Floras from the Southern Guangdong and Guangxi with their Stratigraphic Significance, in *Institute of Vertebrate Paleontology Paleoanthropology and Nanjing Institute of Geology and Paleontology*, Academia Sinica Eds. Mesozoic Cenozoic Red Beds South China (Science Press, 1979), pp. 223–231.
112. Z. Q. Lei, Tertiary sporo-pollen assemblage of Zhujiangkou (Pearl River North) Basin and its stratigraphical significance. *Acta Bot. Sin.* **27**, 94–105 (1985).
113. J. H. Jin, W. B. Liao, B. S. Wang, S. L. Peng, Paleodiversification of the environment and plant community of Tertiary in Hainan Island. *Acta Ecol. Sin.* **22**, 425–432 (2002).
114. J. Y. Xie, J. Li, W. Mai, H. L. Zhang, K. Cai, X. Liu, Palynofloras and age of the Liushagang and Weizhou formations in the Beibuwan Basin, South China Sea. *Acta Palaeontol. Sin.* **51**, 385–394 (2012).
115. X. J. Sun, M. X. Li, Y. Zhang, Z. Lei, Z. C. Kong, P. Li, Q. Qu, Q. Liu, Spores and pollen, in *Tertiary Palaeontology of North Continental Shelf of the South China Sea,* South Sea Branch of Petroleum Corporation of the People's Republic of China, Ed. (Guangdong Science & Technology Press, 1981), pp. 1–58.
116. X. J. Sun, Z. C. Kong, M. X. Li, P. Li, Palynoflora of the Weizhou formation (Eocene-Early Oligocene) in the northern part of South China Sea. *Acta Phytotaxon. Sin.* **19**, 186–194 (1981).
117. Z. Y. Zhang, X. Liu, X. Li, J. Y. Zhang, X. Ke, Y. D. Xu, The Late Oligocene—Early Pleistocene sporopollen assemblages and paleovegetation succession of core ZkA01 in Hetou town, Leizhou Peninsula of Guangdong Province. *Geol. Bull. China* **39**, 880–892 (2020).
118. G. N. Aleksandrova, T. M. Kodrul, J. H. Jin, Palynological and paleobotanical investigations of Paleogene sections in the Maoming basin, South China. *Stratigr. Geol. Correl.* **23**, 300–325 (2015).
119. Z. S. Ning, T. Zhou, Y. Hu, in *Tertiary in Petroliferous Regions of China, VII. The Yunnan–Guanxi region* (Petroleum Industry Press, 1994), pp. 1–193.
120. S. R. Yang, Paleocene Palynology of the Shangyang Formation, Hepu Basin, Guangxi, China. *Acta Micropalaeontol. Sin.* **10**, 213–222 (1993).
121. J. H. Zhang, Discovery of old Tertiary flora from Panxian of Guizhou and its significance, in *Paper of Stratigraphy and Palaeontology of Guizhou*, Committee of Stratigraphy and Paleontology–Geological Society of Guizhou Province Ed. (People's Publishing House of Guizhou, 1983), pp. 133–141.
122. J. R. Tao, Tertiary plants of China, in *Tertiary System of China*, Y. Li, Ed. (Geological Publishing House, 1984), pp. 314–317.
123. J. R. Tao, N. Q. Du, Neogene flora of Tengchong basin in western Yunnan, China. *Acta Bot. Sin.* **24**, 273–281 (1982).
124. Z. C. Song, Late Cenozoic palyno-flora from Zhaotong, Yunnan. *Mem. Nanjing Inst. Geol. Palaeontol. Acad. Sin.* **24**, 1–41 (1988).
125. J. R. Tao, Z. C. Kong, The fossil florule and sporo-pollen assemblage of Shang-in coal series of Erhyuan, Yunnan. *Acta Bot. Sin.* **15**, 120–126 (1973).
126. Y.-J. Huang, T. Su, Z.-K. Zhou, Late Pliocene diversity and distribution of *Drynaria* (Polypodiaceae) in western Yunnan explained by forest vegetation and humid climates. *Plant Divers.* **38**, 194–200 (2016).
127. S. X. Guo, An Eocene flora from the Relu Formation in Litang County of Sichuan and the history of *Eucalyptus*, in *Studies in Qinghai-Xizang Plateau. Special issue of Hengduan Mountains Scientific Expedition II*, Anonymous, Ed. (Beijing Science & Technology Press, 1986), pp. 66–70.
128. Z. C. Song, M. Y. Li, Eocene palynological assemblages from the Gonjo Formation in eastern Xizang. in Regional Geological Surveying Team of Sichuan Geological Bureau, Nanjing Institute of Geology and Palaeontology, Chinese Academy of Sciences Eds. Stratigraphy and palaeontology in West Sichuan and East Xizang, China, part 2 (Sichuan People's Publishing House, 1982) pp. 7–28.
129. G. C. Geng, J. R. Tao, Tertiary plants from Xizang. in *Ser. Sci. Exped. to Qinghai-Xizang Plateau Palaeontology Xizang* (Science Press, 1982), pp. 110–123.
130. Z.-K. Zhou, Q.-S. Yang, K. Xia, Fossils of *Quercus* sect. *Heterobalanus* can help explain the uplift of the Himalayas. *Chin. Sci. Bull.* **52**, 238–247 (2007).
131. Z. C. Song, J. L. Liu, The Tertiary Sporo-Pollen Assemblage from Namling of Xizang, *Ser. Sci. Exped. to Qinghai-Xizang Plateau Palaeontol. Xizang* (Science Press, 1982), pp. 123–145.
132. J. R. Tao, Succession of the floras in Xizang during Upper Cretaceous-Paleogene and Neogene. *Acta Bot. Sin.* **2**, 140–146 (1981).
133. A. M. Fang, Z. Yan, X. H. Liu, J. R. Tao, J. Li, Y. S. Pan, The flora of the Liuqu Formation in south Tibet and its climatic implications. *Acta Palaeontol. Sin.* **44**, 442 (2005).
134. J. Hsu, J. R. Tao, X. J. Sun, On the discovery of a *Quercus semicarpifolia* bed at Mount Shisha Pangma and its significance in botany and geology. *Acta Bot. Sin.* **15**, 102–112 (1973).
135. Y. H. Zheng, Sporo-pollen assemblage of the Wuoma Formation of the Gyrong Basin, in *Team of Comprehensive Scietific Expedition to the Qinghai–Xizang Plateau*, Academia Sinica, Ed. Quaternary Geology in Xizang, (Science Press, 1983), pp. 145–152.
136. J. Li, Y. Zhou, Palaeovegetation type analysis of the late Pliocene in Zanda basin of Tibet. *J. Palaeogeogr.* **14**, 52–58 (2001).
137. L. Cao, Pliocene palynological flora in Disong of Burang, Xizang (Tibet). *Acta Palaeontol. Sin.* **21**, 469–484 (1982).
138. T. Deng, F. Wu, Z. Zhou, T. Su, Tibetan Plateau: An evolutionary junction for the history of modern biodiversity. *Sci. China Earth Sci.* **63**, 172–187 (2020).
139. Z. C. Kong, L. Liu, N. Q. Du, Discussion on Uplift of Tibet Plateau During Late Tertiary and Quaternary based on Pollen Data from Kunlun–Tanggula Mountains, in *Uplift, Age, Amplitude and Form of Uplift of Tibet Plateau* (Science Press, 1981), pp. 77–88.
140. Z. H. Zhu, L. Wu, P. Xi, Z. C. Song, Y. Y. Zhang, *A Research on Tertiary Palynology from the Qaidam Basin, Qinghai Province* (Pet. Ind. Press, 1985), pp. 1–297.
141. C. X. Huang, Y. L. Liang, Sporo-Pollen Analysis on the Lacustrine Deposit in North Part of the Northern Xizang Plateau, in *Team of Comprehensive Scietific Expedition to the Qinghai–Xizang Plateau*, Academia Sinica, Ed., Quaternary Geology in Xizang (Science Press, 1983), pp. 153–161.
142. Z. C. Song, W. M. Wang, F. Y. Mao, Palynological implications for relationship between aridification and monsoon climate in the Tertiary of NW China. *Acta Palaeontol. Sin.* **47**, 265–272 (2008).
143. D.-N. Wang, X.-Y. Sun, Y.-N. Zhao, Late cretaceous to tertiary palynofloras in Xinjiang and Qinghai, china. *Rev. Palaeobot. Palynol.* **65**, 95–104 (1990).
144. S. X. Guo, Z. H. Sun, H. M. Li, Y. W. Dou, Paleocene megafossil flora from Altai of Xinjiang. *Bull. Nanjing Inst. Geol. Palaeontol. Acad. Sin.* **8**, 119–146 (1984).
145. Y. Z. Ma, Tertiary sporo-pollen assemblages from southern Dunhuang basin, Gansu Province. *Acta Micropalaeontologica Sin.* **8**, 207–225 (1991).
146. J. Ma, The tertiary sporopollen assemblage in the Jiuquan basin and the palaeoenvironment. *Pet. Geol. Expeiment* **15**, 423–435 (1993).
147. Y. Z. Ma, X. M. Fang, J. J. Li, F. L. Wu, J. Zhang, Vegetational and environmental changes during late Tertiary–early Quaternary in Jiuxi Basin. *Sci. China Series D* **34**, 107–116 (2004).
148. F. Yang, W. S. Tang, J. M. Wei, Z. Y. Bo, S. J. Liang, *Tertiary in Petroliferous Regions of China, vol. II: The Northwestern Region of China* (Petroleum Industry Press, 1994), pp. 1–253.
149. Z. C. Song, D. H. Zhang, Geological age of the Caomuhao Gypsum Mine in Otog Banner, Nei Mongol with review of research on fossil proteaceous pollen in China. *Acta Palaeontol. Sin.* **29**, 257–269 (1990).
150. S. Y. Sun, Oligocene spore and pollen assemblages from the Tongxin District of Ningxia. *Bull. Inst. Geol. Chin. Acad. Geol. Sci.* **4**, 127–138 (1982).
151. J. Yu, H. Zhang, Q. Lin, Y. Gu, Z. Z. Zhang, Geological implications of sporopollenites flora from Tertiary Xining group in Minhe County, Qinghai Province. *Earth Sci. China Univ. Geosci.* **28**, 401–406 (2003).
152. X. Y. Sun, Y. N. Zhao, Z. S. He, The Oligocene-Miocene palynological assemblages from the Xining-Minghe Basin, Qinghai Province. *Geol. Rev.* **30**, 207–216 (1984).
153. S. X. Guo, Miocene flora in Zekog county of Qinghai. *Acta Palaeontol. Sin.* **19**, 406–411 (1980).
154. J. R. Tao, A late Eocene florula from the district Weinan of central Shensi. *Acta Bot. Sin.* **13**, 272–278 (1965).
155. X. Sun, Z. Qing, Y. Fan, C. Deng, Cenozoic sporo-pollen assemblage of the Weihe Basin, Shaanxi. *Bull. Inst. Geol. Chinese Acad. Geol. Sci.* **9**, 84–109 (1980).
156. L. Zhao, H. Lu, L. Tang, Cenozoic palynological records and vegetation evolution in the Weihe Basin, Central China. *Quat. Sci.* **38**, 1083–1093 (2018).
157. G. W. Liu, D. Y. Li, F. Huang, Q. L. Fu, A Pliocene flora from the Gantang Formation of Yuanmou Basin, Yunnan Province, SW China and its paleoclimate significance. *Acta Palaeontol. Sin.* **41**, 1–9 (2002).
158. G. W. Liu, Late Cenozoic palynological sequence of Eastern Qinghai-Xizang Plateau and its bearing on palaeogeography. *Acta Micropalaeontologica Sin.* **13**, 363–372 (1996).
159. S. X. Guo, J. L. Chen, Cenozoic floras and coal-accumulating environment in Himalayas and Hengduan mountains areas. *Acta Palaeontol Sin.* **28**, 512–521 (1989).
160. B. Y. Geng, J. R. Tao, G. P. Xie, Early Tertiary fossil plants and paleoclimate of Lanzhou Basin. *Acta Phytotaxon. Sin.* **39**, 105–115 (2001).
161. Y. Z. Ma, J. J. Li, X. M. Fan, Pollen-based vegetational and climatic records during 30.6 to 5.0 My from Linxia area, Gansu. *Chin. Sci. Bull.* **43**, 301–304 (1998).
162. G. Wu, J. Qin, S. Mao, Deep-water Oligocene pollen record from South China Sea. *Chin. Sci. Bull.* **48**, 2511 (2003).
163. S. Yi, S. Yi, D. J. Batten, H. Yun, S.-J. Park, Cretaceous and Cenozoic non-marine deposits of the Northern South Yellow Sea Basin, offshore western Korea: Palynostratigraphy and palaeoenvironments. *Palaeogeogr. Palaeoclimatol. Palaeoecol.* **191**, 15–44 (2003).
164. N. M. Makulbekov, Paleogene flora of Southern Mongolia. *Work. Jt. Paleontol. Exped. USSR Mong.* **35**, 8–57 (1988).
165. Q.-Q. Zhang, D. K. Ferguson, V. Mosbrugger, Y.-F. Wang, C.-S. Li, Vegetation and climatic changes of SW China in response to the uplift of Tibetan Plateau. *Palaeogeogr. Palaeoclimatol. Palaeoecol.* **363–364**, 23–36 (2012).
166. S.-F. Li, L.-M. Mao, R. A. Spicer, J. Lebreton-Anberrée, T. Su, M. Sun, Z.-K. Zhou, Late Miocene vegetation dynamics under monsoonal climate in southwestern China. *Palaeogeogr. Palaeoclimatol. Palaeoecol.* **425**, 14–40 (2015).
167. F. M. B. Jacques, S.-X. X. Guo, T. Su, Y.-W. W. Xing, Y.-J. J. Huang, Y.-S. C. Liu, D. K. Ferguson, Z.-K. K. Zhou, Quantitative reconstruction of the Late Miocene monsoon climates

of southwest China: A case study of the Lincang flora from Yunnan Province. *Palaeogeogr. Palaeoclimatol. Palaeoecol.* **304**, 318–327 (2011).
168. L.-B. Jia, Y.-J. Huang, H. Sun, T. Su, J. Huang, Z.-K. Zhou, First fossil of *Pterolobium* (Leguminosae) from the Middle Miocene Yunnan, South China. *Rev. Palaeobot. Palynol.* **242**, 21–32 (2017).
169. Y. Xing, T. Utescher, F. M. B. Jacques, T. Su, Y. C. Liu, Y. Huang, Z. Zhou, Paleoclimatic estimation reveals a weak winter monsoon in southwestern China during the late Miocene: Evidence from plant macrofossils. *Palaeogeogr. Palaeoclimatol. Palaeoecol.* **358–360**, 19–26 (2012).
170. Y.-J. Huang, L.-B. Jia, T. Su, H. Zhu, A. Momohara, Z.-J. Gu, Z.-K. Zhou, A warm-temperate forest of mixed coniferous type from the upper Pliocene Sanying Formation (southeastern edge of Tibetan Plateau) and its implications for palaeoecology and palaeoaltimetry. *Palaeogeogr. Palaeoclimatol. Palaeoecol.* **538**, 109486 (2020).
171. T. Su, F. M. B. Jacques, R. A. Spicer, Y.-S. Liu, Y.-J. Huang, Y.-W. Xing, Z.-K. Zhou, Post-Pliocene establishment of the present monsoonal climate in SW China: Evidence from the late Pliocene Longmen megaflora. *Clim. Past Discuss.* **9**, 1675–1701 (2013).
172. B.-N. Sun, J.-Y. Wu, Y.-S. Liu, S.-T. Ding, X.-C. Li, S.-P. Xie, D.-F. Yan, Z.-C. Lin, Reconstructing Neogene vegetation and climates to infer tectonic uplift in western Yunnan, China. *Palaeogeogr. Palaeoclimatol. Palaeoecol.* **304**, 328–336 (2011).
173. X. Xu, Climatic and ecological implications of Late Pliocene palynoflora from Longling, Yunnan, China. *Quat. Int.* **117**, 91–103 (2004).
174. J. Wu, K. Zhang, Y. Xu, G. Wang, C. N. Garzione, J. Eiler, P. H. Leloup, P. Sorrel, G. Mahéo, Paleoelevations in the Jianchuan Basin of the southeastern Tibetan Plateau based on stable isotope and pollen grain analyses. *Palaeogeogr. Palaeoclimatol. Palaeoecol.* **510**, 93–108 (2018).
175. G. Dupont-Nivet, C. Hoorn, M. Konert, Tibetan uplift prior to the Eocene-Oligocene climate transition: Evidence from pollen analysis of the Xining Basin. *Geology* **36**, 987–990 (2008).
176. C. F. Chen, *Cenozoic pollen records and Palaoenvironmental evolution in Xining Basin, Northeastern Tibetan Plateau* (Masteral Diss. China Lanzhou Univ., 2009), pp. 1–1344.
177. Y. F. Miao, X. M. Fang, Z. C. Song, F. L. Wu, W. X. Han, S. Dai, C. H. Song, Late Eocene pollen records and palaeoenvironmental changes in northern Tibetan Plateau. *Sci. China Ser. D Earth Sci.* **51**, 1089–1098 (2008).
178. A. F. Xiao, D. P. Li, H. J. Zhang, X. L. Li, Climate evolution and composional features of sporopollen in the Oligocene–pliocene series of the Kumukuli Basin in Xinjiang. *Geol Shaanxi* **21**, 36–44 (2003).
179. W. M. Wang, J. W. Shu, Late cenozoic palynofloras from Qujing basin, Yunnan, China. *Acta Palaeontol. Sin.* **43**, 254–261 (2004).
180. Z. H. Wu, W. Jiang, D. Nelson, B. Kidd, Strata and spores association of Dogai Coring redbeds of North Tibetan Plateau. *Geoscience* **16**, 225–230 (2002).
181. Y. Ma, F. Wu, X. Fang, J. Li, Z. An, W. Wang, Pollen record from red clay sequence in the central Loess Plateau between 8.10 and 2.60 Ma. *Chin. Sci. Bull.* **50**, 2234–2243 (2005).
182. L. Wang, H. Y. Lü, N. Q. Wu, J. Li, Y. P. Pei, G. B. Tong, S. Z. Peng, Palynological evidence for Late Miocene–Pliocene vegetation evolution recorded in the red clay sequence of the central Chinese Loess Plateau and implication for palaeoenvironmental change. *Palaeogeogr. Palaeoclimatol. Palaeoecol.* **241**, 118–128 (2006).
183. Z. S. Ji, X. De Yang, W. Zang, J. X. Yao, Z. H. Wu, New palynological materials from the Shexing Formation in the Lhasa Block, Tibet, and their stratigraphic significance. *Acta Geosci. Sin.* **23**, 323–328 (2002).
184. X.-Y. Kou, D. K. Ferguson, J.-X. Xu, Y.-F. Wang, C.-S. Li, The reconstruction of paleovegetation and paleoclimate in the Late Pliocene of West Yunnan, China. *Clim. Change* **77**, 431–448 (2006).
185. R.-P. Lu, P. Luo, J.-E. Han, J. Yu, Q.-W. Meng, Z.-G. Shao, D.-G. Zhu, X.-G. Meng, Features of the sporopollen assemblage at the Toling section in the Zanda basin, Tibet, China, and its paleoclimatic significance. *Geol. Bull. China* **25**, 1475–1480 (2006).
186. M.-x. Dong, F.-l. Li, D.-z. Gao, M.-s. Geng, L.-y. Li, A study of the late Miocene dry event based on sporo-pollen variations in Sunitezuoqi, Inner Mongolia. *Acta Geosci. Sin.* **27**, 207–212 (2006).
187. X. P. Guo, N. W. Wang, X. Z. Ding, Palaeontological proof of the naij tal group-complex as mélange aggregation in the eastern kunlun orogenic belt and its geologic significance. *Geol. Rev.* **52**, 289–294 (2006).
188. X. P. Guo, N. W. Wang, D. N. Wang, X. Z. Ding, M. Zhao, Discovery of Miocene sporopollen from Matrix Strata of the Naij Tal Group-complex in the Eastern Kunlun orogenic belt. *Geol. Rev.* **53**, 824–831 (2007).
189. J. Sun, Q. Xu, B. Huang, Late Cenozoic magnetochronology and paleoenvironmental changes in the northern foreland basin of the Tian Shan Mountains. *J. Geophys. Res.* **112**, B04107 (2007).
190. F. Wu, X. Fang, Y. Ma, M. Herrmann, V. Mosbrugger, Z. An, Y. Miao, Plio–Quaternary stepwise drying of Asia: Evidence from a 3-Ma pollen record from the Chinese Loess Plateau. *Earth Planet. Sci. Lett.* **257**, 160–169 (2007).
191. Q. F. Duan, K. X. Zhang, J. X. Wang, H. Z. Yao, J. J. Pu, Sporopollen assemblage from the Totohe Formation and its stratigraphic significance in the Tanggula Mountains, northern Tibet. *Earth Sci. China Univ. Geosci.* **32**, 623–637 (2007).
192. J.-W. Shu, W.-M. Wang, E. B. Leopold, J.-S. Wang, D.-S. Yin, Pollen stratigraphy of coal-bearing deposits in the Neogene Jidong Basin, Heilongjiang Province, NE China: New insights on palaeoenvironment and age. *Rev. Palaeobot. Palynol.* **148**, 163–183 (2008).
193. J. Sun, Z. Zhang, Palynological evidence for the mid-Miocene climatic optimum recorded in Cenozoic sediments of the Tian Shan Range, northwestern China. *Glob. Planet. Change* **64**, 53–68 (2008).
194. X. M. Fang, F. L. Wu, W. X. Han, Y. D. Wang, X. Z. Zhang, W. L. Zhang, Plio-Pleistocene drying process of Asian inland—sporopollen and salinity records from Yahu section in the central Qaidam Basin. *Quat. Sci.* **28**, 874–882 (2008).
195. J. G. Li, Y. Y. Zhang, H. W. Cai, Z. Y. Guo, X. Q. Wan, Cretaceous and Paleogene palynological successions at Zhongba. *Acta Geol. Sin.* **82**, 584–593 (2008).
196. Q. F. Duan, K. X. Zhang, J. X. Wang, H. Z. Yao, Z. J. Niu, Oligocene palynoflora, paleovegetation and paleoclimate in the Tanggula Mountains, Northern Tibet. *Acta Micropalaeontologica Sin.* **25**, 185–195 (2008).
197. J.-F. Li, D. K. Ferguson, J. Yang, G.-P. Feng, A. G. Ablaev, Y.-F. Wang, C.-S. Li, Early Miocene vegetation and climate in Weichang District, North China. *Palaeogeogr. Palaeoclimatol. Palaeoecol.* **280**, 47–63 (2009).
198. J. G. Li, Z. Y. Guo, Y. Y. Zhang, Palynofloral assemblages from the Dagzhuka Formation at Qiabulin, Xigaze, Xizang (Tibet): Their age and bearing on palaeoenvironments and palaeogeography. *Acta Palaeontol. Sin.* **48**, 163–174 (2009).
199. W. M. Wang, T. Deng, Palynoflora from the stratotype section of the Neogene Xiejian stage and its significance. *Acta Palaeontol. Sin.* **48**, 1–8 (2009).
200. J. F. Li, Y. Q. Hu, D. K. Ferguson, Y. F. Wang, C. Sen Li, An Early Pliocene lake and its surrounding vegetation in Zhejiang, East China. *J. Paleolimnol.* **43**, 751–769 (2010).
201. C. Quan, Z. Zhou, Occurrence of Oligocene *Ginkgo* megafossils from Heilongjiang Province and its paleophytogeographic significance. *Acta Paleontol. Sin.* **49**, 439–442 (2010).
202. F. F. Sun, W. Y. Zhang, J. C. Gong, C. J. Zhang, The palaeoenvironmental reconstruction on pollen proxy in the Qaidam Basin since Late Pliocene. *Geol. Rev.* **56**, e628 (2010).
203. Y. D. Xu, K. X. Zhang, G. C. Wang, S. Y. Xiang, S. S. Jiang, F. N. Chen, Geological Significance of Miocene-Early Pleistocene Palynological Zones in the Gyirong Basin, Southern Tibet. *Earth Sci.* **35**, 759–773 (2010).
204. X. R. Li, X. M. Fang, F. L. Wu, Y. F. Miao, Pollen evidence from Baode of the northern Loess Plateau of China and strong East Asian summer monsoons during the Early Pliocene. *Chin. Sci. Bull.* **56**, 64–69 (2011).
205. J. Lu, B. Song, R. Chen, J. Zhang, H. Ye, Palynological assemblage of Eocene-Oligocene pollen and their biostratigraphic correlation in Dahonggou, Daqaidam Regions, Qaidam Basin. *Earth Sci. J. China Univ. Geosci.* **35**, 839–848 (2010).
206. Z. Hui, J. Li, Q. Xu, C. Song, J. Zhang, F. Wu, Z. Zhao, Miocene vegetation and climatic changes reconstructed from a sporopollen record of the Tianshui Basin, NE Tibetan Plateau. *Palaeogeogr. Palaeoclimatol. Palaeoecol.* **308**, 373–382 (2011).
207. M. A. Khan, R. Ghosh, S. Bera, R. A. Spicer, T. E. V. Spicer, Floral diversity during Plio-Pleistocene Siwalik sedimentation (Kimin formation) in Arunachal Pradesh, India, and its palaeoclimatic significance. *Palaeobiodivers. Palaeoenviron.* **91**, 237–255 (2011).
208. Y. Miao, X. Fang, M. Herrmann, F. Wu, Y. Zhang, D. Liu, Miocene pollen record of KC-1 core in the Qaidam Basin, NE Tibetan Plateau and implications for evolution of the East Asian monsoon. *Palaeogeogr. Palaeoclimatol. Palaeoecol.* **299**, 30–38 (2011).
209. F. Qin, D. K. Ferguson, R. Zetter, Y. Wang, S. Syabryaj, J. Li, J. Yang, C. Li, Late Pliocene vegetation and climate of Zhangcun region, Shanxi, North China. *Glob. Chang. Biol.* **17**, 1850–1870 (2011).
210. Z. Tang, Z. Ding, P. D. White, X. Dong, J. Ji, H. Jiang, P. Luo, X. Wang, Late Cenozoic central Asian drying inferred from a palynological record from the northern Tian Shan. *Earth Planet. Sci. Lett.* **302**, 439–447 (2011).
211. Z. Zhang, J. Sun, Palynological evidence for Neogene environmental change in the foreland basin of the southern Tianshan range, northwestern China. *Glob. Planet. Change.* **75**, 56–66 (2011).
212. M. Cai, X. Fang, F. Wu, Y. Miao, E. Appel, Pliocene–Pleistocene stepwise drying of Central Asia: Evidence from paleomagnetism and sporopollen record of the deep borehole SG-3 in the western Qaidam Basin, NE Tibetan Plateau. *Global Planet. Change* **94**, 72–81 (2012).
213. H. Hao, D. K. Ferguson, H. Chang, C.-S. Li, Vegetation and climate of the Lop Nur area, China, during the past 7 million years. *Clim. Change* **113**, 323–338 (2012).
214. J.-W. Shu, W.-M. Wang, A Miocene pollen flora from the petroliferous deposits in the Bohai Bay Basin, North China, and its palaeoclimatic and stratigraphic significance. *Palaeoworld* **22**, 109–118 (2013).
215. J. Sun, X. Ni, S. Bi, W. Wu, J. Ye, J. Meng, B. F. Windley, Synchronous turnover of flora, fauna, and climate at the Eocene–Oligocene Boundary in Asia. *Sci. Rep.* **4**, 7463 (2014).
216. J. Sun, Q. Xu, W. Liu, Z. Zhang, L. Xue, P. Zhao, Palynological evidence for the latest Oligocene–early Miocene paleoelevation estimate in the Lunpola Basin, central Tibet. *Palaeogeogr. Palaeoclimatol. Palaeoecol.* **399**, 21–30 (2014).
217. C. B. Wan, Y. W. Sun, Y. F. Xue, X. Y. Qiao, Y. D. Jin, Y. Y. Zhang, Neogene palynological assemblages in the west slope of Songliao Basin and their geological implications. *Sci. China Earth Sci.* **57**, 2486–2497 (2014).

218. X. F. Xia, N. Zhang, J. X. Yu, C. Yi, Eocene-Oligocene palynology and biostartigraphic correlation in the Nanpu Sag, Bohai Bay Basin, North China. *Acta Micropalaeontologica Sin.* **32**, 269–284 (2015).
219. J. Yang, Y. Qin, Q. Xu, X. Zhou, Y. Hu, D. Du, L. Meng, Palaeovegetation evolution features of the Tianjin coastal region since 7.65Ma BP. *Acta Geol. Sin.* **89**, 1134–1143 (2015).
220. Y. Yang, P. H. Jin, C. Dong, X. Xu, R. Li, F. Ma, Q. Wang, Y. Miao, B. Sun, Palynological assemblage from the Late Miocene of Tiantai-Ninghai area, Zhejiang, China and its paleovegetation and paleoclimate. *Quat. Sci.* **35**, 669–682 (2015).
221. X. Zhao, C. Zhang, H. Wu, X. Ren, L. Chang, Z. Guo, Significance of Eocene-Oligocene transition pollen record from Xining Basin, China. *Quat. Sci.* **35**, 1489–1499 (2015).
222. L. J. Wei, X. H. Liu, G. W. Li, X. J. Zhou, Paleogene palynological assemblages and paleoenvironmental analysis from Gyachala formation in the Gyangzi area, Southern Tibet, China. *Acta Micropalaeontologica Sin.* **32**, 255–268 (2015).
223. J. Liu, J. J. Li, C. H. Song, H. Yu, T. J. Peng, Z. C. Hui, X. Y. Ye, Palynological evidence for late Miocene stepwise aridification on the northeastern Tibetan Plateau. *Clim. Past* **12**, 1473–1484 (2016).
224. Q.-t. Meng, A. A. Bruch, G. Sun, Z.-j. Liu, F. Hu, P.-c. Sun, Quantitative reconstruction of Middle and Late Eocene paleoclimate based on palynological records from the Huadian Basin, northeastern China: Evidence for monsoonal influence on oil shale formation. *Palaeogeogr. Palaeoclimatol. Palaeoecol.* **510**, 63–77 (2018).
225. Z. Hui, J. Li, C. Song, J. Chang, J. Zhang, J. Liu, S. Liu, T. Peng, Vegetation and climatic changes during the Middle Miocene in the Wushan Basin, northeastern Tibetan Plateau: Evidence from a high-resolution palynological record. *J. Asian Earth Sci.* **147**, 116–127 (2017).
226. Q. Yuan, V. Vajda, Q.-K. Li, Q.-S. Fan, H.-C. Wei, Z.-J. Qin, X.-R. Zhang, F.-S. Shan, A late Eocene palynological record from the Nangqian Basin, Tibetan Plateau: Implications for stratigraphy and paleoclimate. *Palaeoworld* **26**, 369–379 (2017).
227. Y. F. Zhang, D. S. Liu, X. H. Zhang, Neogene palynological assemblages from Qiongdongnan Basin and their paleoclimatic implications. *Mar. Geol. Quat. Geol.* **37**, 93–101 (2017).
228. P. R. Bai, Y. R. Zeng, Y. S. Li, Z. M. Liao, D. S. Ma, H. B. Fu, C. H. Mo, H. Guo, H. F. Fan, Y. S. Yang, Discovery and its significance of the eocene plant fossils in the kongnongla. Area from the Southeast Margin Bangor Basin in Northern Tibet. *Guizhou Geol. Surv.* **34**, 301–305 (2017).
229. T. Ying, D. Shaw, S. Schneider, Oligocene fossil assemblages from Lake Nanning (Yongning Formation; Nanning Basin, Guangxi Province, SE China): Biodiversity and evolutionary implications. *Palaeogeogr. Palaeoclimatol. Palaeoecol.* **505**, 100–119 (2018).
230. Y. Li, Z. Zhang, G. Ding, Q. Xu, Y. Wang, Z. Chi, J. Dong, L. Zhang, Late Pliocene and early Pleistocene vegetation and climate change revealed by a pollen record from Nihewan Basin, North China. *Quat. Sci. Rev.* **222**, 105905 (2019).
231. B. I. Pavlyutkin, T. I. Petrenko, I. Y. Chekryzhov, V. P. Nechaev, T. A. Moore, The plant biostratigraphy of the Cenozoic coal-bearing formations in Primorye, Russian Far East. *Int. J. Coal Geol.* **220**, 103414 (2020).
232. K. Ai, G. Shi, K. Zhang, J. Ji, B. Song, T. Shen, S. Guo, The uppermost Oligocene Kailas flora from southern Tibetan Plateau and its implications for the uplift history of the southern Lhasa terrane. *Palaeogeogr. Palaeoclimatol. Palaeoecol.* **515**, 143–151 (2019).
233. D. Zheng, G. Shi, S. R. Hemming, H. Zhang, W. Wang, B. Wang, S.-C. Chang, Age constraints on a Neogene tropical rainforest in China and its relation to the Middle Miocene Climatic Optimum. *Palaeogeogr. Palaeoclimatol. Palaeoecol.* **518**, 82–88 (2019).
234. W. M. Wang, G. J. Chen, Y. F. Chen, G. D. Kuang, Tertiary palynostratigraphy of the Ningming basin, Guangxi. *J. Stratigr.* **27**, 324–327 (2003).
235. J. Huang, T. Su, S. Li, F. Wu, T. Deng, Z. Zhou, Pliocene flora and paleoenvironment of Zanda Basin, Tibet, China. *Sci. China Earth Sci.* **63**, 212–223 (2020).
236. Q. Li, X. Zhou, X. Ni, B. Fu, T. Deng, Latest Middle Miocene fauna and flora from Kumkol Basin of northern Qinghai-Xizang Plateau and paleoenvironment. *Sci. China Earth Sci.* **63**, 188–201 (2020).

Acknowledgments: We thank D. Beerling for allowing access to the code for the SDGVM, G. J. L. Tourte from the University of Bristol for help on climate modeling techniques, P. Liu from Xishuangbanna Tropical Botanical Garden (XTBG), Chinese Academy of Sciences (CAS) for the help on fossil data collection, and three anonymous reviewers for many comments and suggestions. **Funding:** This work was supported by the NSFC-RCUK NERC joint project (no. 41661134049), the grant of Natural Environment Research Council (no. NE/P013805/1), National Natural Science Foundation of China (no. 41772026 to S.L. and no. 31470325 to T.S.), the Strategic Priority Research Program of CAS (no. XDA20070301 to Z.Z.), Yunnan Province Natural Science Foundation (2019FB061), XTBG International Fellowship for Visiting Scientists to R.A.S., Key Research Program of Frontier Sciences, CAS (no. QYZDB-SSW-SMC016 to T.S.), Youth Innovation Promotion Association, CAS (no. 2017439 to T.S.), and the CAS 135 program (no. 2017XTBG-F01 to T.S.). **Author contributions:** S.-F.L. P.J.V., A.F., and Z.-K.Z. designed the research plan. S.-F.L., P.J.V., A.F., and T.D.-B. carried out the simulations. S.F.L., T.S., J.L., J.H., H.T., W.-Y.-D.D., L.-L.C., and Z.-K.Z. collected fossil data. S.-F.L., P.J.V., A.F., and Z.-K.Z performed analysis. S.-F.L. and P.J.V. wrote the first draft of the paper. S.-F.L., P.J.V., A.F., D.J.L., R.A.S., T.S., and Z.-K.Z. revised the manuscript. All authors discussed and commented on the manuscript. **Competing interests:** The authors declare that they have no competing interests. **Data and materials availability:** All data needed to evaluate the conclusions in the paper are present in the paper and/or the Supplementary Materials. Model data can be accessed at http://bridge.bris.ac.uk/resources/simulations. Additional data related to this paper may be requested from the authors.

Submitted 31 May 2020
Accepted 4 December 2020
Published 27 January 2021
10.1126/sciadv.abc7741

Citation: S.-F. Li, P. J. Valdes, A. Farnsworth, T. Davies-Barnard, T. Su, D. J. Lunt, R. A. Spicer, J. Liu, W.-Y.-D. Deng, J. Huang, H. Tang, A. Ridgwell, L.-L. Chen, Z.-K. Zhou, Orographic evolution of northern Tibet shaped vegetation and plant diversity in eastern Asia. *Sci. Adv.* **7**, eabc7741 (2021).

Science Advances

Orographic evolution of northern Tibet shaped vegetation and plant diversity in eastern Asia

Shu-Feng Li, Paul J. Valdes, Alex Farnsworth, T. Davies-Barnard, Tao Su, Daniel J. Lunt, Robert A. Spicer, Jia Liu, Wei-Yu-Dong Deng, Jian Huang, He Tang, Andy Ridgwell, Lin-Lin Chen and Zhe-Kun Zhou

Sci Adv **7** (5), eabc7741.
DOI: 10.1126/sciadv.abc7741